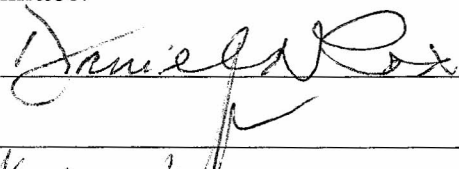


MICRORNA-MEDIATED REGULATORY CONTROL OF CLASS SPECIFIC
DENDRITE MORPHOGENESIS IN *DROSOPHILA*

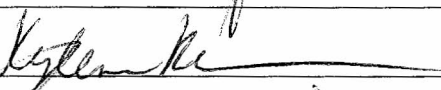
by

Shruthi Sivakumar
A Thesis
Submitted to the
Graduate Faculty
of
George Mason University
in Partial Fulfillment of
The Requirements for the Degree
of
Master of Science
Biology

Committee:



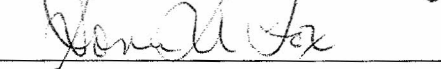
Dr. Daniel N. Cox, Thesis Director



Dr. Ancha Baranova, Committee Member



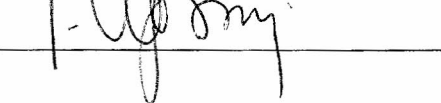
Dr. Kyle Kehn-Hall, Committee Member



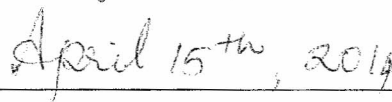
Dr. James D. Willett, Department Chair



Dr. Donna M. Fox, Associate Dean,
Associate Dean for Academic Affairs,
College of Science



Dr. Peggy Agouris, Dean, College of
Science

Date: 

Spring Semester 2014
George Mason University
Fairfax, VA

MicroRNA-mediated regulatory control of class specific dendrite morphogenesis in
Drosophila

A thesis submitted in partial fulfillment of the requirements for the degree of Master of
Science at George Mason University

By

Shruthi Sivakumar
Bachelor of Technology
Anna University, 2009

Committee Chair: Daniel N. Cox, Associate Professor
School of Systems Biology, Krasnow Institute for Advanced Study

Spring Semester 2014
George Mason University
Fairfax, VA

Copyright 2014, Shruthi Sivakumar
All Rights Reserved

DEDICATION

To Dr. Daniel N. Cox for giving me this opportunity that has changed my life and taken me in a completely new direction. Thank you for your generosity in sharing with me your knowledge and lab resources in order to make this thesis successful.

ACKNOWLEDGEMENTS

I am fortunate to be part of a lab with an intense collaborative atmosphere that has allowed me to experiment and grow without boundaries. I am indebted to my Advisor and Mentor, Dr. Daniel N. Cox for encouraging me and introducing me to new opportunities.

I would also like to extend my sincere thanks to the committee members Dr. Ancha Baranova and Dr. Kylene Kehn-Hall for agreeing to serve on my committee and for their valuable time.

I have had a great time working with the entire microRNA team: Srividya Chandramouli Iyer, Ramakrishna Meduri, Myurajan Rubaharan, Atit Patel, Francis Aguisanda for the stimulating discussions and for the sleepless nights we had when working together to achieve deadlines.

My special thanks to Sarah A. Trunnell for being a supportive friend and for donation of the two-color cytoskeleton reporter strain and also Surajit Bhattacharya for conducting the Bioinformatic analysis.

I also extend my thanks to all my colleagues of the Cox Lab for their continued support to make this thesis a success.

TABLE OF CONTENTS

List of Figures	vii
List of Tables	viii
List of Abbreviations	ix
Abstract	xi
Chapter One: Introduction	14
1.1 MicroRNAs	14
1.2 Evolutionarily conserved miRNAs in <i>C.elegans</i> , <i>D. melanogaster</i> and <i>H. sapiens</i>	15
1.3 microRNA biogenesis pathway and regulation.....	17
1.4 MicroRNA Target Prediction Tools.....	19
1.4.1 Target Scan	19
1.4.2 Miranda.....	20
1.4.3 PITA (Possibility of interaction by Target Accessibility)	20
1.5 Importance of microRNAs in the Nervous system	21
1.6 Significance of studying the <i>Drosophila</i> Peripheral Nervous System.....	23
1.7 Morphological classification of PNS Neurons.....	24
1.8 Characterization of Class-Specific da neurons.....	26
1.9 <i>GAL4-UAS</i> Binary expression system.....	29
1.10 Mosaic Analyses with a Repressible Cell Marker (MARCM)	31
1.11 Preliminary studies	33
1.12 Specific Aims	36
1.13 Research Plan	37
Chapter Two: Experimental procedures	39
2.1 <i>Drosophila</i> strains and culture	39
2.2 UAS-miRNA Transgenes.....	40
2.3 Gain-of-function Analyses	40
2.4 MARCM Analyses	41
2.5 Larval preparation and live image confocal microscopy	41
2.6 Semi-automated digital reconstruction and quantitative analyses of dendritic morphology	42
2.7 Bioinformatic analyses of miR cluster targets	42
Chapter Three: Results.....	44
3.1 Functional miRNome analyses reveal complex miRNA regulation of class-specific dendrite morphogenesis.....	44

3.1.1 miRNA-mediated promotion of dendritic growth and branching	44
3.1.2 miRNA-mediated restriction of dendritic growth and branching.....	48
3.1.3 Quantitative analyses of miRNA-mediated dendrite morphogenesis.....	52
3.2 The <i>miR-12/283/304</i> cluster functions in fine-tuning class-specific dendritic diversity	54
3.3 Overexpression analyses reveal distinct functional roles of miRNA cluster components.....	59
Chapter Four: Discussions	68
4.1 miRNome analyses reveal complex functional roles for miRNAs in mediating class- specific dendritic development.....	68
4.2 Funcional analyses of the <i>miR12/283/304</i> miRNA cluster	69
List of References	73

LIST OF FIGURES

- Figure 1: Venn diagram representing evolutionarily conserved miRNAs across species
- Figure 2: miRNA biogenesis pathway and the action of the RISC complex on target mRNA degradation or translational repression
- Figure 3: Crystal structure of Argonaute protein from *P. furiosus*
- Figure 4: Organization of the intragenic miRNA cluster *miR-12/283/304* which maps to the fifth intron of the host gene *dGmap* on the X chromosome of the *Drosophila* genome
- Figure 5: *Drosophila* abdominal peripheral nervous system
- Figure 6: *Drosophila* da neurons
- Figure 7: Distribution of da neurons in larval hemi-segment
- Figure 8: Dendritic coverage of body wall by da neurons
- Figure 9: *GAL4-UAS* binary expression system in *Drosophila*
- Figure 10: Schematic illustration of the loss-of-function (LOF) MARCM system
- Figure 11: Disruption of the miRNA pathway results in defects in class-specific dendrite morphogenesis
- Figure 12: Experimental pipeline and map of specific aims
- Figure 13: miR-mediated promotion of dendritic growth/branching in class I da neurons
- Figure 14: miR-mediated promotion of dendritic growth/branching in class III da neurons
- Figure 15: miR-mediated promotion of dendritic growth/branching in class IV da neurons
- Figure 16: miR-mediated repression of dendritic growth/branching in class I da neurons
- Figure 17: miR-mediated repression of dendritic growth/branching in class III da neurons
- Figure 18: miR-mediated repression of dendritic growth/branching in class IV da neurons
- Figure 19: Quantitative analyses of dendritic morphologies
- Figure 20: Summary of neuromorphometric digital reconstructions of da neurons by class for the miRNome genetic screen
- Figure 21: MARCM analyses implicate the *miR-12/283/304* cluster in cell autonomously regulating higher order dendritic branching and overall growth in class III and IV da neurons
- Figure 22: MARCM analyses reveal differential roles for the *miR-12/283/304* cluster in mediating higher order dendritic branching and growth in class I and II da neurons
- Figure 23: Overexpression analyses reveal differential and opposing roles for miR cluster components
- Figure 24: Overexpression analyses strongly implicate *miR-12* in promoting class-specific dendritic diversity
- Figure 25: *miR-12* mediated regulation of dendritic arborization

LIST OF TABLES

Table 1: Comparative neurometric analyses implicate *miR-12* in promoting dendritic diversity and regulation of class III-specific arborization characteristics

LIST OF ABBREVIATIONS

AGO	Argonaute
bp	basepairs
<i>C. elegans</i>	<i>Caenorhabditis elegans</i>
Chr	Chromosome
CNS	Central Nervous system
<i>Cos2</i>	costal-2
<i>Cyo</i>	Curly of Oster
<i>D. melanogaster</i>	<i>Drosophila melanogaster</i>
Da neuron	<i>Drosophila</i> dendritic arborization neuron
dbd	dorsal bd
Dcr-1	dicer-1
Dcr-2	dicer-2
ddaA	dorsal cluster class III da neuron
ddaB	dorsal cluster class II da neuron
ddaC	dorsal cluster class IV da neuron
ddaD	dorsal cluster class I da neuron
ddaE	dorsal cluster class I da neuron
ddaF	dorsal cluster class III da neuron
dFMR1	drosophila fragile X mental retardation protein 1
dmd1	dorsal md 1 neuron
DNA	Deoxyribonucleic acid
<i>Dpp</i>	decapentaplegic
FLP	flippase enzyme
FMRP	fragile x mental retardation protein
FRT	flippase recognition target
<i>Fu</i>	<i>fused</i>
GFP	green fluorescent protein
GMA	GFP fused to actin binding domain of Moesin
<i>Gmap</i>	Golgi microtubule -protein
GOF	Gain-of-function
<i>H. sapiens</i>	<i>Homo sapiens</i>
HEK293	Human Embryonic Kidney cells
hs	heat shock promoters
ldaA	lateral cluster class II da neuron
ldaB	lateral cluster class III da neuron
LOF	Loss-of-function
MARCM	Mosaic analysis with a repressible Cell marker
mCD8	mouse cluster of differentiation 8
MCM6	DNA replication licensing
MCT1	monocarboxylate transporter
miR	micro RNA
miRNA	micro RNA
mRNA	messenger RNA
nt	nucleotide
<i>P.furiosus</i>	<i>Pyrococcus furiosus</i>

PAZ	Piwi Argonaute Zwiller
PIWI	P-element induced wimpy testis in <i>Drosophila</i>
<i>Pka-C1</i>	cAMP-dependent protein kinase 1
PNS	Peripheral nervous system
<i>Ppk</i>	<i>Drosophila pickpocket gene</i>
Pre-miRNA	precursor-microRNA
Pri-miRNA	primary-microRNA
Ran-GTP	RNAs-related Nuclear protein-GTP
RFP	Red fluorescent protein
rhoA	Ras homolog gene family -A
RISC	RNA-induced silencing complex
RN3	Ribonuclease3
RNA	Ribonucleic acid
RNA pol II	RNA polymerase II
RNAi	RNA interference
RNP	Ribonucleoprotein
siRNA	silencing RNA
<i>Smo</i>	smoothened
SNARE	SNAP receptor complex
<i>Syb</i>	Synaptobrevin
tubP	tubulin-P
UAS	Upstream Activating Sequence
UTR	Untranslated region
VAMP	Vesicle-associated membrane protein
v'ada	ventral' cluster neuron Class IV da neuron
v'pda	ventral' cluster neuron Class III da neuron
vdaA	ventral cluster neuron Class III da neuron
vdaB	ventral cluster neuron Class IV da neuron
vdaC	ventral cluster neuron Class III da neuron
vdaD	ventral cluster neuron Class III da neuron
vpda	ventral cluster neuron Class I da neuron
<i>w</i>	<i>Drosophila white gene</i>
<i>y</i>	<i>Drosophila yellow gene</i>

ABSTRACT

MICRORNA-MEDIATED REGULATORY CONTROL OF CLASS SPECIFIC DENDRITE MORPHOGENESIS IN *DROSOPHILA*

Shruthi Sivakumar, M.S.

George Mason University, 2014

Thesis Director: Dr. Daniel N. Cox

Dendrites function as the primary sites of synaptic and sensory input and integration in the developing nervous system. Moreover, numerous cognitive disorders such as Autism, Rett's syndrome, Angelman's syndrome and Schizophrenia are associated with dendritic abnormalities including development and maintenance (Kaufmann and Moser, 2000). MicroRNAs (miRNAs) have recently emerged as critical post-transcriptional regulators of gene expression in numerous tissues, particularly the nervous system, with functions in specification of neuronal development, formation and maintenance of dendritic fields, neuronal asymmetry, axonal and dendrite targeting and local translation at synapses based on neuronal activity. Despite the aforementioned advances, the precise role of miRNA-mediated regulation of neuronal morphogenesis and development of class specific dendrite arborization patterns remains largely unknown. The peripheral nervous system (PNS) of *Drosophila melanogaster* provides an excellent system in which to elucidate the molecular mechanisms governing class specific dendrite morphogenesis and homeostasis using dendritic arborization (da) sensory neurons as a model system. Based on the central hypothesis that *miRNA-mediated post-transcriptional regulation is required for establishing and/or maintaining distinct class specific dendritic*

morphologies, the studies described herein focus on large-scale, comparative morphological analyses of the roles of miRNAs in mediating class-specific da sensory neuron dendrite development via miRNome-directed gain-of-function genetic screens and corresponding loss-of-function mutant analyses. To assess the biological significance of these deregulated miRNA phenotypes, it is important to examine whether these gain-of-function effects are relevant to native endogenous gene function. To directly address this question, we elected to analyze a particular miRNA cluster, composed of *miR-12*, *miR-283* and *miR-304* (*miR-12/283/304* cluster) via both mutant and overexpression phenotypic analyses. Expression analyses reveal that *miR-12* and *miR-304* are differentially enriched in complex class III and IV da neurons relative to the morphologically simple class I neurons. MARCM mutant analyses implicate the *miR-12/283/304* cluster in cell autonomously regulating higher order dendritic branching, particularly the formation of actin-rich dendritic filopodia, as well as in promoting overall dendritic growth. To dissect the individual contributions of miRNA cluster components, we conducted overexpression studies which revealed differential roles for these miRNAs in mediating class-specific dendritic diversity. Overexpression studies indicate that *miR-12*, and to a lesser extent *miR-304*, act in a similar direction to promote dendritic growth and branching, especially actin-rich filopodia, whereas *miR-283* acts to restrict these processes such that with full cluster overexpression there is an intermediate phenotype reflective of the opposing functional roles of these miRNAs in mediating class III dendrite morphogenesis. Intriguingly, while the same regulatory effects of these miRNAs were observed in class IV neurons, we found that overexpression of *miR-12* in these neurons resulted in the *de novo* formation of actin rich filopodia and produced a shift in class IV neurons towards class III arborization characteristics indicating that regulated expression of members of this miRNA cluster is important for promoting class-specific dendritic diversity.

Collectively, these studies provide both global insight and a robust foundation on the importance of miRNAs in mediating class specific dendrite morphogenesis and will potentially shed novel light on the molecular mechanisms via which miRNA regulation underscores such biologically relevant events as learning and memory, as well as nervous system disease pathologies.

CHAPTER ONE: INTRODUCTION

Dendrites are the key specialized structures that represent the information input centers of the neuron and play functional roles in the establishment and maintenance of proper neuronal circuitry (Arikkath, 2012; Jan and Jan, 2010). In order to ensure proper neuronal function, several critical factors need to be taken into account including dendritic field specification, stereotypic branching patterns, density of dendrites and modulation during development (Jan and Jan, 2010). The stereotypic arborization pattern of dendritic morphology is regulated by a wide variety of molecular mechanisms, including cytoskeletal regulation, cell signaling, the secretory pathway and transcriptional regulation, all of which play essential roles in achieving class-specific dendrite homeostasis. Moreover, a broad spectrum of neurological and cognitive disorders including Rett syndrome, Fragile X syndrome, Alzheimer's disease and Parkinson's disease are linked to disruptions in dendritic morphology and neural connectivity at dendritic spines (Arikkath, 2012; Yu and Lu, 2012). For example, Fragile X syndrome is caused by loss-of-function mutations in the *FMRP* gene which acts as a negative translational regulator by associating with components of the miRNA pathway including the Dicer and Argonaute proteins (Duan and Jin, 2006).

1.1 MicroRNAs

MicroRNAs (miRNAs) represent an important class of endogenous, non-coding RNA molecules, ~21 to 24 nucleotides in length, which act as critical post-transcriptional modulators of gene expression. These molecules form duplexes with their target mRNA transcripts and induce a cleavage or translational repression (Rooij, 2011). They play a critical functional role in regulating gene expression during normal development and in pathological responses (Davis and

Hata, 2009). Moreover, many miRNAs are known to be evolutionarily conserved across species (Ibáñez-Ventoso et al., 2008). One of the first miRNA and mRNA target interactions that was revealed was in *C. elegans*, where the miRNA *lin-4* regulates expression of the *lin-14* gene (Wightman et al., 1993). This was followed by the identification of the second miRNA, *let-7* that repressed the expression of several genes during development (Reinhart et al., 2000). In 2002, researchers revealed that the down-regulation or loss of *miR-15* and *-16* led to the development of leukemia indicating a link between miRNA abundance and human diseases, after which copious data and reports revealed functional relationship between miRNA and target mRNAs (Calin et al., 2002; Huang et al., 2011; Saugstad, 2010).

1.2 Evolutionarily conserved miRNAs in *C.elegans*, *D. melanogaster* and *H. sapiens*

According to the miRBase, there are ~1100 *Homo sapiens*, 233 *Caenorhabditis elegans* and 186 *Drosophila melanogaster* miRNAs found in the microRNA.org website (<http://www.microrna.org/>). The number of mature miRNA sequences has considerably increased from a count of 5,071 in miRBase release 10.1 December 2007 to 24,521 in miRBase release 20 June 2013. Using data from release 10.1, earlier studies (Ibáñez-Ventoso et al., 2008) were conducted on mature miRNA sequences of *C. elegans*, *D. melanogaster* and *H. sapiens* genomes in order to investigate the evolutionary conservation between and within the species which revealed the following:

1. Approximately 87 *C. elegans* miRs are 5' related to 62 *Drosophila* miRs, whereas 31 *C. elegans* miRs have >70% overall similarity to 37 *Drosophila* miRs.
2. Approximately 76 *C. elegans* miRs are 5' related to 98 human miRs, whereas 22 *C. elegans* are > 70% identical over similarity to 46 human miRs.

1.3 microRNA biogenesis pathway and regulation

Within the nucleus, the primary miRNAs (pri-miRNA) transcripts are transcribed from independent miRNA genes via the RNA polymerase II (RNA pol II) enzyme. Several imperfectly base-paired stems and sequences for several different miRNAs are found within a pri-miRNA. The pri-miRNA is cropped, polyadenylated and further subjected to a series of enzymatic reactions in a two-step process involving the RNase III-type endonucleases Drosha (also known as RN3) and Dicer. Drosha and its partner protein Pasha (in *Drosophila*) complex and process the pri-miRNA to form the precursor miRNA (pre-miRNA) producing ~70 nucleotide hairpins. The pre-miRNA that is formed is exported from the nucleus into the cytoplasm via the Ran-GTP mechanism in the presence of Exportin5. The exported pre-miRNA is cleaved with the help of a Dicer to form 21-24 nucleotide miRNA duplexes. This step of pre-processing occurs in the presence of Dcr-1 and partner Loquacious, meanwhile Dcr-2 and its partner R2D2 generates siRNAs (Carthew and Sontheimer, 2009). One strand acts as the mature miRNA and the other strand is degraded. The final stage is the maturation stage where the mature miRNA strand associates with the RISC complex comprised of AGO family proteins, which in turn represses the expression of the target mRNA to which it binds resulting in translational repression or mRNA cleavage (**Fig. 2**). The translational repression occurs when the miRNA seed sequence of ~7-8 nucleotide has an imperfect or partial complementarity with the 3' UTR binding sites of the mRNA sequence whereas when there is a precise complementarity between the seed sequence of miRNA and mRNA sequence, the AGO2 protein within the RISC complex will cleave the mRNA resulting in mRNA degradation (Davis and Hata, 2009; Filipowicz et al., 2008). The components of the miRNA biogenesis pathway therefore play essential roles in translational repression or mRNA degradation (Schmitter et al., 2006). The Argonaute complex, that contains the effector ribonucleoprotein (RNP), associates with the

single stranded miRNA thereby creating a RNA-induced silencing complex (RISC) which recognizes the target mRNA and inhibits protein expression. The Argonaute family of proteins (Ago-1, 2, 3, 4) are comprised of two well conserved functional domains which regulate the 'slicer' activity of the RISC including the PAZ domain and the PIWI domain (Carthew and Sontheimer, 2009; Song et al., 2006) (**Fig. 3**). In eukaryotes, translational initiation requires a combination of the initiator factor 4E and a 7-methylguanosine cap of the mRNA sequence and when the miRNA base pairs with the target mRNA, the RISC complex (Ago proteins) interact with the 7-methylguanosine and thereby block translational initiation (Kiriakidou et al., 2007).

Figure 2: miRNA biogenesis pathway and the action of the RISC complex on target mRNA degradation or translational repression (adapted from Joshi et al., 2011).

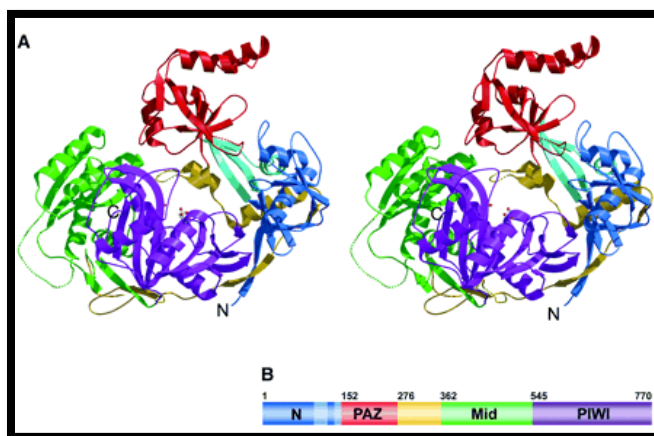
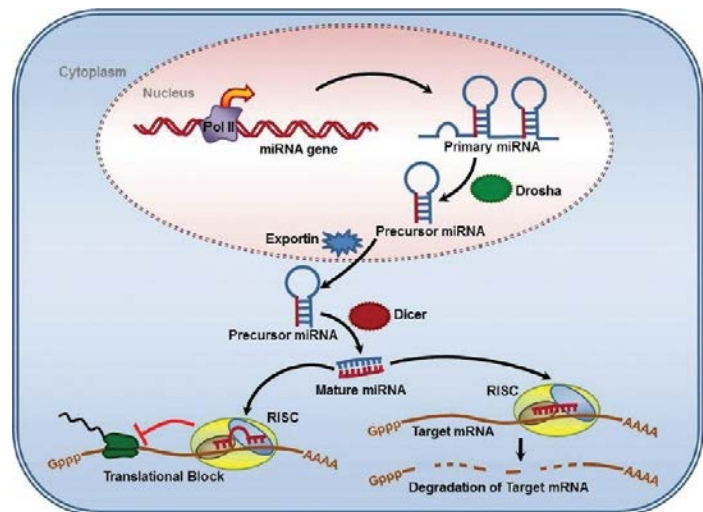


Figure 3: Crystal structure of Argonaute protein from *P. furiosus*. (A) Stereoview ribbon representation of Argonaute protein showing the N-terminal domain (blue), the "stalk" (light blue), the PAZ domain (red), the middle domain (green), the PIWI

domain (purple), and the interdomain connector (yellow). (B) Schematic of domain organization. Image adapted from Song et al. (2004).

Analyses of the effects of down-regulation of Dicer and Ago proteins revealed that among the different members in the Argonaute family, Ago-2 plays a very important role in the miRNA pathway in HEK293 cells (Schmitter et al., 2006). And in *Drosophila*, loading of miRNA and siRNA occurs in different Ago complexes. Another study revealed that Dicer and a component of RISC, eIF2c, were directly involved in association with the Fragile X mental retardation protein (FMRP) thereby regulating synaptogenesis (Lugli et al., 2005).

1.4 MicroRNA Target Prediction Tools

The tools that are used for miRNA target predictions are based on 3 different approaches and are classified as follows (Sturm et al., 2010):

- A. An approach that neither makes use of the seed match requirement, nor the evolutionary conservation across species
- B. Predictions that requires the seed match requirement, but not the conservation
- C. Finally, a combination approach that uses the seed match requirement as well as evolutionary conservation across species

Ideally, the target prediction tool utilizes the complementarity of sequence alignment of seed sequences of the miRNA and the sequence of the mRNA target (3'UTR). Some of the current target prediction tools that are most widely employed are discussed below.

1.4.1 Target Scan

This tool predicts the 8-mer and 7-mer sites and utilizes the perfect sequence complementarity of the miRNA seed region to the target mRNA. This is followed by calculation of the thermodynamic free energy required for the binding between the seed region and putative target and thereby generates a score to each UTR. An improved extended version of the TargetScan is

TargetScan S, which utilizes the 6-mer seed region of a miRNA as well as the surrounding downstream 3' match of adenosine residues to find the potential targets (Lewis et al., 2003; Min and Yoon, 2010).

1.4.2 miRanda

Initially this tool was specifically designed to identify the *Drosophila* miRNA targets, however this tool was later used for analyses of human miRNA targets. The principles that miRanda implements to identify the target genes for a miRNA are the score values of miRNA and mRNA sequence complementarity using a position weighed local algorithm, measurement of the free energy of bonding between the duplex and evolutionary conservation of targets across related species (Enright et al., 2003; Min and Yoon, 2010). A lower free energy value ($\Delta\Delta G < 0$) indicates a favored reaction, and thermodynamic stable bonding between the RNA-RNA duplex calculated using the Vienna package (Kertesz et al., 2007).

1.4.3 PITA (Possibility of interaction by Target Accessibility)

This algorithm is based on RNA-RNA duplex formation considering free energy minimization. The scoring is based on the difference between the free energy that is gained to form the RNA-RNA duplex and free energy lost to unwind the RNA-RNA duplex (Kertesz et al., 2007). Its feature is to investigate the target site accessibility as determined by the base-pairing interaction between the miRNA and mRNA site (Zheng et al., 2013).

1.5 Importance of microRNAs in the Nervous system

MiRNAs are associated with the regulation of many cellular mechanisms and aberrant miRNA expression has been detected in various disease states. MicroRNAs play a pivotal role in the nervous system as first indicated by disruption of the Zebrafish *dicer* gene which led to the suppression the miRNA pathway and concomitant defects in brain morphogenesis (Giraldez et al., 2005). Many *Drosophila* miRNAs are specifically expressed in the embryonic nervous system; for example: *miR-124* is a neural-specific miRNA that is particularly enriched in the CNS, while *miR-279*, the intronic cluster *miR-12/283/304* (**Fig. 4**) and *miR-263b* are known to be expressed in the embryonic peripheral nervous system (Aboobaker et al., 2005).

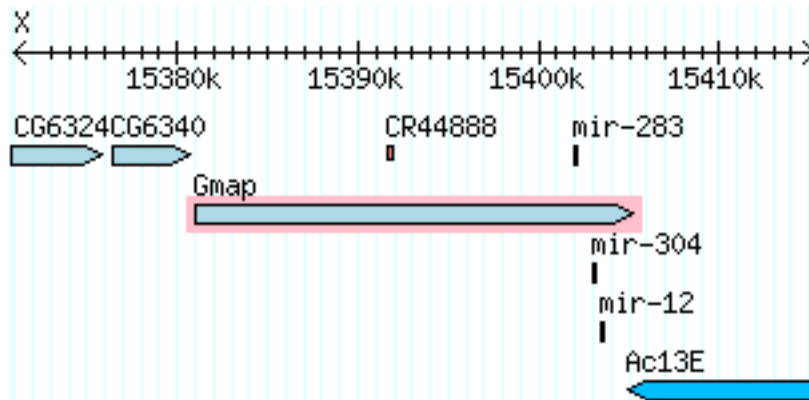


Figure 4: Organization of the intragenic miRNA cluster *miR-12/283/304* which maps to the fifth intron of the host gene *Gmap* on the X chromosome of the *Drosophila* genome. Image adapted from FlyBase (flybase.org).

Relatively few miRNAs that are specifically expressed and enriched in the nervous system have been studied, to date, for their role in regulation of gene expression in biological processes such as learning and memory, neuronal differentiation, synaptic plasticity, neuronal degeneration, as well as neurogenesis. Among these, *miR-9* functions in early neurogenesis and

proliferation and *miR-124* in neuronal differentiation of progenitor cells to mature neurons. Moreover, *miR-124* has been shown to associate with the *Drosophila* homolog of FMRP (dFMR1) resulting in reduced dendritic branching of dendritic arborization sensory neurons. Other studies reveal that *miR-134* represses the translation of a LIM domain protein kinase K in regulating dendritic spine development (Kaur et al., 2012; Schratt et al., 2006; Xu et al., 2008). Despite the compelling evidence provided by different studies of microRNAs on neuronal development and activity of the nervous system (Bejarano et al., 2012; Bian and Sun, 2011; Cochella and Hobert, 2012; Liu et al., 2012; Luikart et al., 2012; Shi et al., 2010), to date no global investigations of miRNA function have been reported at a functional level.

Despite the aforementioned advances, the precise roles of miRNA-mediated regulation of neuronal morphogenesis and development of class specific dendrite arborization remains largely unknown.

1.6 Significance of studying the *Drosophila* Peripheral Nervous System

The larval peripheral nervous system (PNS) of *Drosophila melanogaster* is used as one of the powerful tools to study important questions in neural development including axonal and dendritic growth and morphogenesis, cell division, apoptosis, and cell lineage. The PNS is composed of a vast number of neurons that vary in size, shape, position and connection with other neurons (Bodmer and Jan, 1987). These neurons signal between each other with the help of specialized subcellular thin structures called dendrites and axons. Apart from transmitting signals, they also play an active role in computation and storage of information with the help of the highly stereotypical dendrite arbors (Jan and Jan, 2010). The arrangement of neurons in each hemisegment beneath the transparent cuticle of the insect body occurs in a highly stereotypical pattern and distinct subclasses of sensory neuron can be identified based upon similar dendritic arborization patterns (Grueber et al., 2002, 2005). With the development of specific transgenic reporter systems it is possible to tag individual neuron subtypes with fluorescent markers such as GFP, which allow for *in vivo* analyses of neural development (Gao et al., 1999). Intriguingly, studies of *Drosophila* neurons have revealed a correlation between axonal and dendritic arbor complexity at the class-specific level, *i.e.* neurons which display complex dendritic arbors likewise have complex axonal arbors (Grueber et al., 2007). Several gain-of-function studies on the importance of genes regulating the dendrite outgrowth, development and routing have revealed the molecular mechanisms that govern class specific dendritic morphogenesis (Gao et al., 1999; Ou et al., 2008). Moreover, large-scale genetic screens have revealed that mutations that disrupt dendritic development in a variety of ways (Gao et al., 1999). Also, genetic screens with the help of powerful loss-of-function studies like RNAi, have revealed interesting genes with known and unknown functions, that had direct or indirect effects on the dendritic development (Ivanov et al., 2004; Koizumi et al., 2007; Parrish et al., 2006; Iyer et al., 2013).

1.7 Morphological classification of PNS Neurons

The PNS neurons are classified based on the dendritic branching patterns and the targets they innervate such as 1) es neurons that innervate external sensory structure, 2) ch neurons that innervate chordotonal organs, 3) da neurons that gives rise to multiple dendrites in late embryogenesis, 4) bd neurons that have bipolar dendrites growing in opposite directions and 5) td neurons that activate the tracheal branches (Bodmer and Jan, 1987). The da sensory neurons provide an excellent model system to study neuronal morphogenesis in living preparations as these neurons are located just below the transparent larval body wall (Bodmer and Jan, 1987). The organization and characterization of neurons within the *Drosophila* PNS is based on the three factors: shape, size and dendritic tree branching complexity. These combinations of features enable each neuron to communicate to the surrounding neurons in order to define proper neural circuits and information processing.

In *Drosophila*, each larval hemisegment is comprised of es, ch, da, bd and td neurons and in each hemisegment there are a total of 15 da neurons (**Fig. 5**). *Drosophila* da neurons are further classified into 4 individual morphological subclasses referred to as Class I-IV, which is reflective of the increasing orders of dendritic branching complexity (**Fig. 6**). Class I and II da neurons display relatively simpler dendritic branching complexity compared to classes III and IV where a significant increase in complexity and area of coverage is observed.

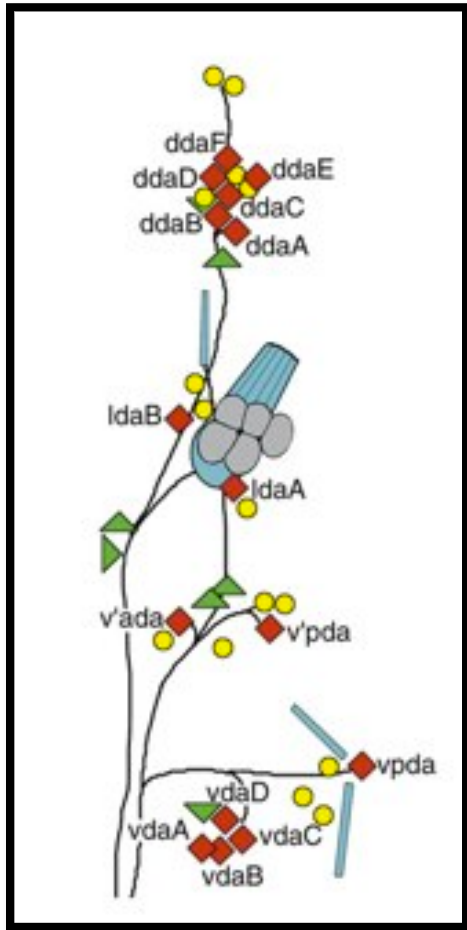


Figure 5: *Drosophila* abdominal peripheral nervous system. Schematic is depicting a single abdominal hemisegment in which da neurons are represented as red diamonds. Image adapted from Grueber et al. (2002).

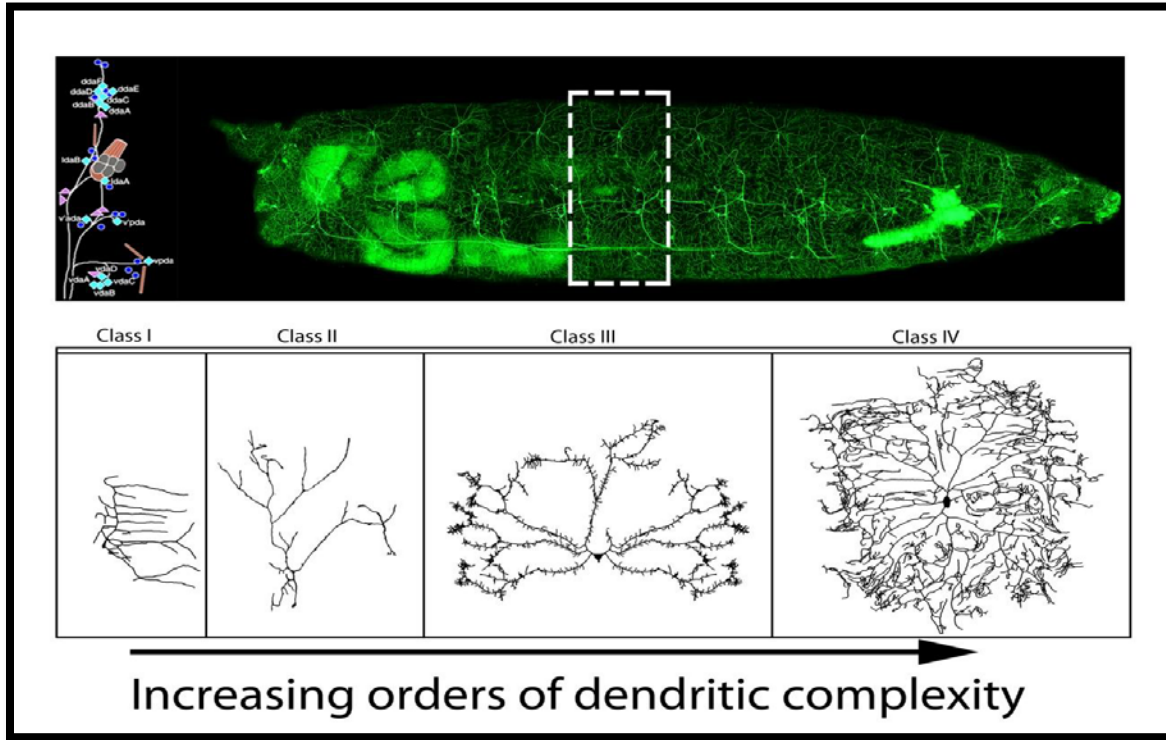


Figure 6: *Drosophila* da neurons. (Top) Lateral view of larva with class IV da neurons labeled with GFP with schematic of da neuron organization shown at left. Schematic is depicting a single abdominal hemisegment in which da neurons are represented as diamonds and color-coded according to morphological classification (Class I-IV) with numbers corresponding to increasing orders of dendritic complexity. (Bottom) Representative images of typical dendritic morphologies observed in Class I-IV da neurons. All images are to scale.

1.8 Characterization of Class-Specific da neurons

Drosophila da neurons spread out extensively across the larval epidermis with a defined stereotypical dendritic morphology and dendritic territory. These da neurons are organized into 4 clusters including ventral, ventral', lateral and dorsal at the ventral, lateral and dorsal regions respectively (**Fig. 7**). The prefix v, v', l or d with an alphabetical suffix, identifies the position of the da neurons within one of the four clusters. Hence, the ventral' and ventral cluster comprises

of 7 neurons such as v'ada and v'pda neurons, and vdaA, vdaB, vdaC, vdaD and vpda, respectively. The lateral cluster comprises of 2 neurons such as ldaA and ldaB. The dorsal cluster incorporates the dorsal set of neurons and they have been labeled as ddaA, ddaB, ddaC, ddaD, ddaE and ddaF (Grueber et al., 2002).

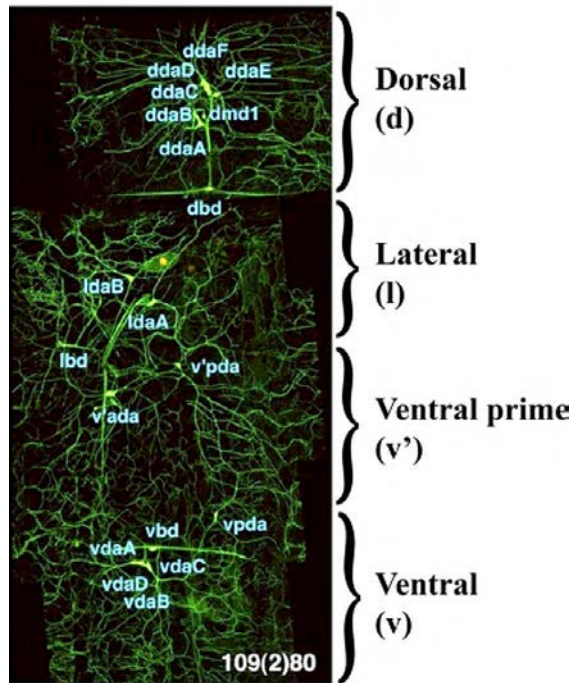


Figure 7: Distribution of da neurons in larval hemi-segment. Confocal image of a larval hemi-segment expressing the pan-da *GAL4*¹⁰⁹⁽²⁾⁸⁰ driving the expression of *UAS-mCD8::GFP* (green) and *UAS-Red Stinger* (red, nuclei). On the right hand side is a breakdown of the dorsal (d), lateral (l), ventral prime (v') and ventral (v) clusters of da neurons. Also labeled in this image are dmd1, dbd, and vbd neurons, which while multi-dendritic do

not belong to the da neuron subclass of the PNS. Image adapted and modified from Hughes and Thomas (2007).

Drosophila Class I da neurons within each larval abdominal hemisegment are comprised of 3 neurons, ddaD and ddaE located in the dorsal region and vpda located in the ventral region. These class I neurons display the simplest dendritic branching architecture (Grueber et al., 2002). The dendrites are smooth, with a main primary dendrite and a few secondary dendrites projecting from it. Class II da neurons are comprised of vdaA and vdaC innervating the ventral region of each hemisegment, ldaA in lateral region and ddaB in the dorsal body wall. These 4 neurons have long dendrites and are more symmetrically bifurcated relative to the class I

dendrites. The most abundant of the four classes of neurons are the Class III neurons, which include vdaD, v'pda, ldaB, ddaA and ddaF. These Class III neurons have a higher branching complexity than either Class I or II, and are characterized by long primary and secondary branches with characteristic spiked protrusions (dendritic filopodia, 1-20µm) rich in actin and lacking stable microtubules (Grueber et al., 2002; Jan and Jan, 2010). Moreover, Class III neurons exhibit properties of dendritic tiling and collectively the dendritic arbors of Class III neurons cover ~70% of the body wall in a non-overlapping pattern within each abdominal hemisegment. Class IV neurons are comprised of vdaB, v'ada and ddaC and these neurons display the most complex dendritic branching pattern, and like Class III neurons exhibit dendritic tiling properties with nearly complete, and non-overlapping dendritic coverage of the larval body wall within each hemisegment (Grueber et al., 2002) (**Fig. 8**).

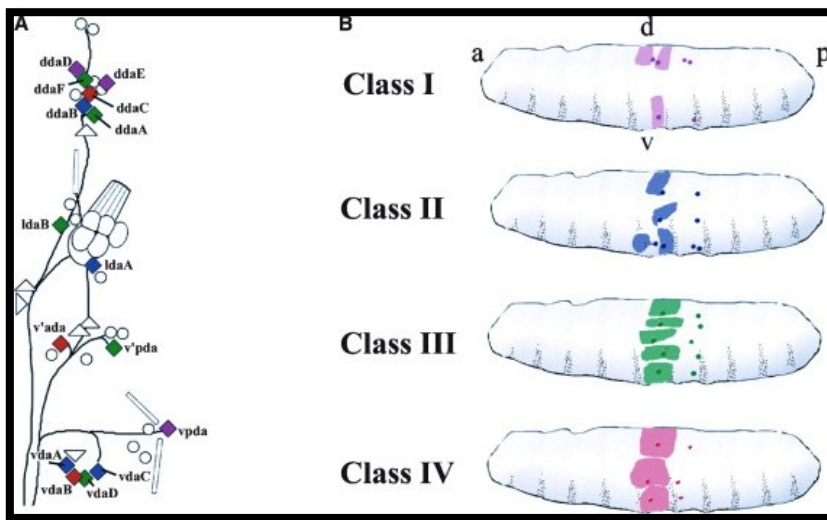


Figure 8: Dendritic coverage of body wall by da neurons.

A) Color coded diamond shaped da neurons have been placed in the same morphological class. (B) Larvae diagram represents the distribution of neurons and the

dendritic coverage across the larval body wall for the 4 distinct morphological classes of da neurons. Image adapted from (Jan and Jan, 2010)

1.9 *GAL4-UAS* Binary expression system

The *GAL4-UAS* system is a versatile tool developed in order to study targeted gene expression in *Drosophila* (Duffy, 2002). This genetic method regulates the temporal and spatial expression of genes making it possible to investigate *in vivo* gene function with exceptionally high resolution. This system tagged with fluorescent proteins like GFP and RFP provides a system for visualizing dendrite development in *Drosophila* da neurons. Further, the use of distinct *GAL4* drivers for specific classes of da neurons makes it possible to visualize and analyze dendrite morphogenesis of individual da neuron subclasses, as well as perturb individual gene function, throughout developmental stages of interest. Comparison of this data with the wild-type control provides the necessary information of the role of the mutation of interest in the *Drosophila* PNS. GAL4 is a modular protein consisting of a DNA binding and transcriptional activation domain. It is obtained from yeast, consisting of 881 amino acids. In the presence of galactose, GAL4 activation leads to the regulation of *GALI* and *GALI10* genes by binding to the four 17 bp sites defined as an Upstream Activating Sequence (UAS), thereby resulting in the transcriptional activation of the GAL4-regulated genes (Giniger et al., 1985). GAL4 performs the DNA binding activity at the first 74 residues whereas transcriptional activations maps to two regions 148-196 and 761-88. Further, the GAL4 controlled expression of the UAS drives the expression of the reporter genes that are tagged to the fluorescent proteins such as GFP or RFP (UAS-GFP) and located at a region downstream of the upstream activating site (UAS) sequence within the *Drosophila* genome (Duffy, 2002; Fischer et al., 1988). This bipartite system thereby requires 2 main components, the responder line and the other termed as a driver line. The driver line consists of the yeast transcriptional activator, GAL4 and the responder line is the UAS sequence located upstream of a desired gene of interest, to which the GAL4 specifically binds to activate gene transcription. Both components are required to achieve gene expression in specific tissues

(e.g. PNS) and the absence of one of the components such as GAL4 would result the responder line to remaining in a silent state. Hence, in order to activate transcription, transgenic flies expressing GAL4 in a specific pattern, recognized as the driver, are mated to flies bearing the UAS element, known as the responder lines. This results in a progeny with the expression of responder genes in a pattern respective to the GAL4 driver line (Brand and Perrimon, 1993; Duffy, 2002) (**Fig. 9**).

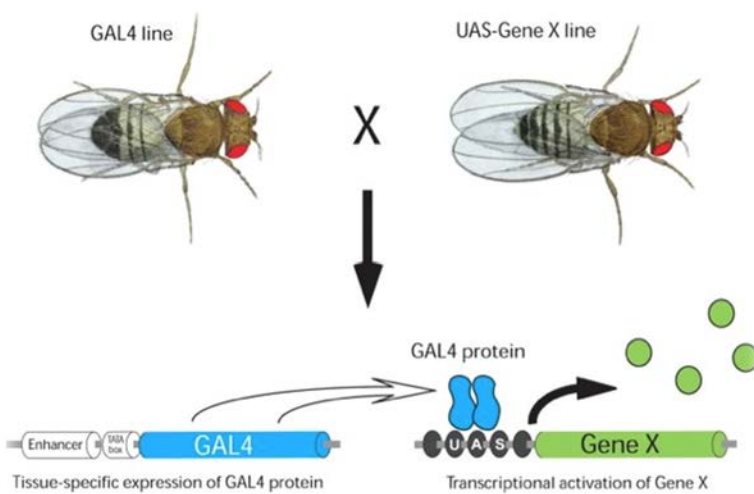


Figure 9: GAL4-UAS binary expression system in *Drosophila*. When flies carrying a UAS responder (e.g. *UAS-GFP*) are mated to flies carrying a GAL4 driver, progeny containing both elements of the system are produced. This method of gene

expression leads to the activation of Gene X in a wide variety of tissue and cell-specific patterns
Image adapted from Southall et al. (2008).

Specific GAL4 lines unique to da neurons subclasses are now available enabling class-specific analyses and visualization of dendrite morphogenesis further making it possible to investigate the functional relevance of genes in class-specific dendrite development and homeostasis. Some of these GAL4 drivers include *GAL4²²¹*, which expresses predominantly in Class I da neurons (Grueber et al., 2003) and *ppk-GAL4*, which expresses specifically in Class IV da neurons (Grueber et al., 2007). Recently, a database was developed by collecting image data for 6,650 GAL4 driver lines in *Drosophila* adult brain and ventral nerve cord, which will be

an advantageous resource in neuroanatomical studies and neural circuit dissection (Jenett et al., 2012).

1.10 Mosaic Analyses with a Repressible Cell Marker (MARCM)

MARCM analyses represents a novel genetic method for investigating the cell autonomous role of gene function by inducing the formation of homozygous mutant cell clones in an otherwise heterozygous mutant background. As such, this system enables one to produce single cell mutant clones for mutations which may otherwise be lethal prior to the desired stage of development or the formation of a cell-type of interest for analyses (Lee and Luo, 2001; Wu and Luo, 2006; Kao and Lee, 2012). Importantly, these clones are marked with a live-cell marker (GFP) which allows the direct analysis of the mutant phenotype for the gene of interest in a specific cell type (for example, the PNS). Meanwhile, the presence of GAL80, a small protein from yeast results in the repression of the function of GAL4 genes, thereby inhibiting the expression of GFP and producing unmarked cells that are heterozygous for both GAL80 and mutation. The key tools in this genetic technique are the flippase (FLP) recombinase/ FRT recombination target system mediating mitotic recombination and the other, the ability to mark the homozygous mutant cells. Collectively, the mosaic analysis focuses on the generation of homozygous mutant cells that are positively labeled by GFP from heterozygous precursors via a mitotic recombination in an unlabeled animal (**Fig. 10**). The major applications of generation of genetic mosaics are (**A**) to conduct functional analyses of candidate genes by understanding whether the gene functions cell-autonomously in a specific tissue or cell type of interest, for example; RhoA, a GTPase protein known to regulate actin cytoskeleton is required cell autonomously for the restriction of dendritic growth and proliferation of neuroblasts (Lee et al., 2000); (**B**) for cell lineage analyses; (**C**) genetic screens of gene function in a given cell-type;

(D) to investigate the stage of lethality for a mutation of interest; or (E) to study the functional role of an embryonically lethal mutation by generation of heterozygous cells surrounding the homozygous mutant clone.

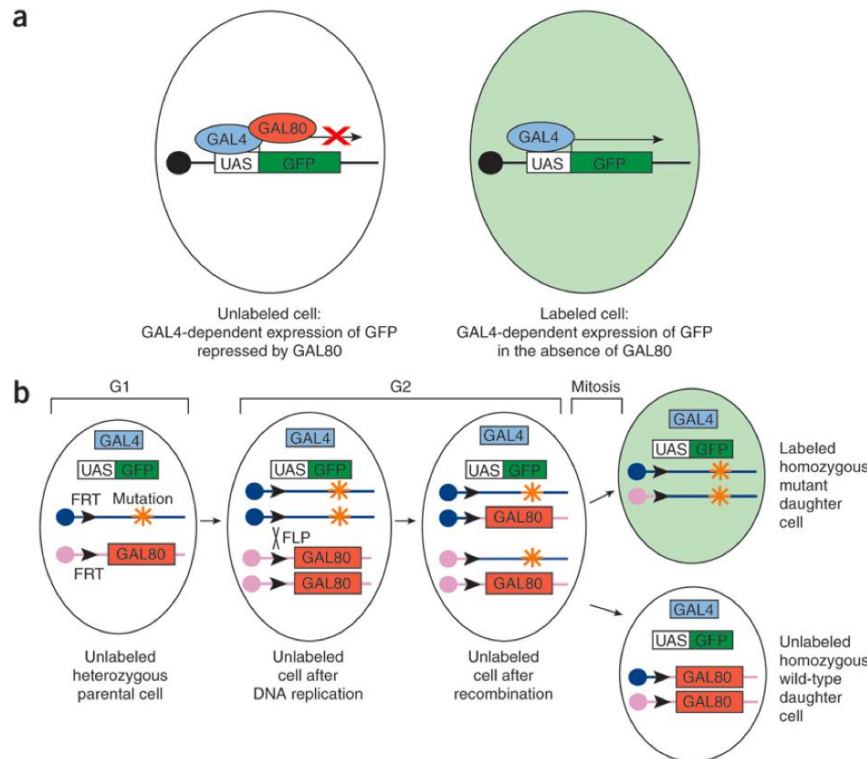


Figure 10: Schematic illustration of the loss-of-function (LOF) MARCM system. (a) In cells containing the GAL80 protein, GAL4-dependent expression of a UAS-gene (GFP) is repressed. By contrast, cells containing GAL4 but lacking GAL80 will express the UAS-gene (GFP). In this schematic,

genes are denoted by colored boxes whereas proteins are denoted by colored ovals. (b) LOF MARCM requires two FRT sites located at the same position on homologous chromosomes; GAL80 located distal to one of the FRT sites; FLP recombinase located anywhere in the genome; GAL4 located anywhere in the genome except distal to the FRT site on the FRT, GAL80 recombinant chromosome arm; UAS-marker located anywhere in the genome except distal to the FRT site on the FRT, GAL80 recombinant chromosome arm; and optionally a mutation distal to FRT, in trans to but not on the FRT, GAL80 recombinant chromosome arm. Site-specific mitotic recombination at FRT sites (black arrowheads) gives rise to two daughter cells, each of which is homozygous for the chromosome arm distal to the FRT sites. Ubiquitous expression of GAL80 represses GAL4-dependent expression of a UAS-marker (GFP) gene. Loss of GAL80 expression in homozygous mutant cells results in specific expression of GFP. Adapted directly from Wu and Luo (2007).

1.11 Preliminary Studies

The dendritic arborization (da) sensory neurons of the *Drosophila* peripheral nervous system offer an excellent model system for elucidating the molecular mechanisms governing class specific dendrite morphogenesis and for exploring miRNA-mediated control of this process (**Fig. 6**). To determine whether miRNA regulation was essential in da neuron dendrite development, we performed loss-of-function studies of two key components of the miRNA biogenesis machinery, *dicer-1* and *Ago-1* and these studies clearly revealed strong phenotypic effects on dendrite morphogenesis indicating that miRNAs likely play important roles in specifying class-specific dendrite arborization patterns (**Fig. 11**). To facilitate functional analyses of miRNA regulation in da neurons, we have previously conducted whole-genome miRNA expression profiling as well as mRNA expression profiling of three distinct classes of da neurons, thereby generating a comprehensive molecular gene expression signature within these individual subclasses of da neurons (**Fig. 12A, B, C**). For this miRNome profiling, total RNA (including miRNAs) was extracted from class I, III, and IV da neuron subpopulations via a magnetic bead based cell-sorting method developed in the Cox Laboratory (Iyer et al., 2009) (**Fig. 12B**). This method allows for rapid and specific cell enrichment using antibody-coated magnetic beads. The isolated RNA is of high quality and can be efficiently used for genome, miRNome and proteome analyses. The results of the expression matrix obtained from the profiling revealed that selected miRNAs were detected in all the 3 da neuron subclasses, whereas other miRNAs displayed differential expression patterns among class I, III and IV neurons suggesting potential cell-type specific regulatory roles for mediating class-specific dendritic homeostasis. The analyses revealed 75 significantly expressed miRNAs in the da neuron subclasses and differential expression for many of these miRNAs. The heat map presented below consists of the top 30 miRNAs that displayed differential expression across the

three classes of da neurons analyzed (**Fig. 12C**).

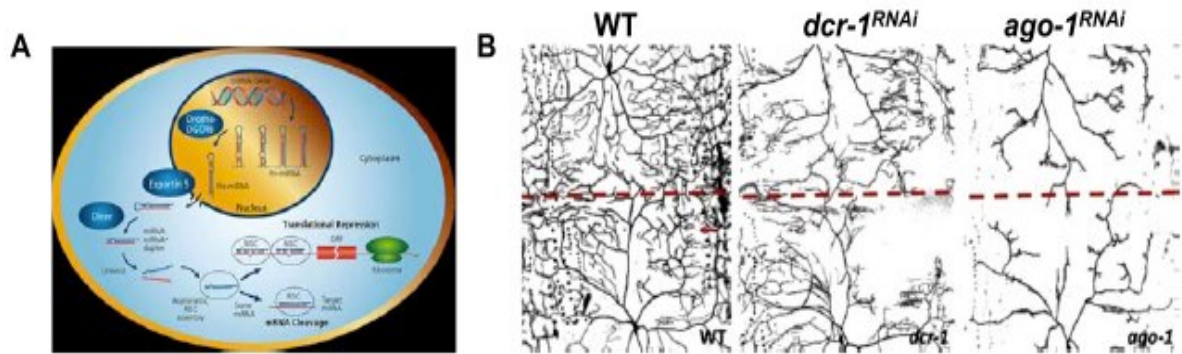


Figure 11. Disruption of the miRNA pathway results in defects in class-specific dendrite morphogenesis. (A) Schematic diagram of miRNA pathway. (B) Disruption of *dcr-1* and *ago-1* result in dendrite defects, including reduced branching complexity and field coverage in class IV da neurons suggesting that miR regulation likely plays a critical role in mediating class-specific dendrite homeostasis.

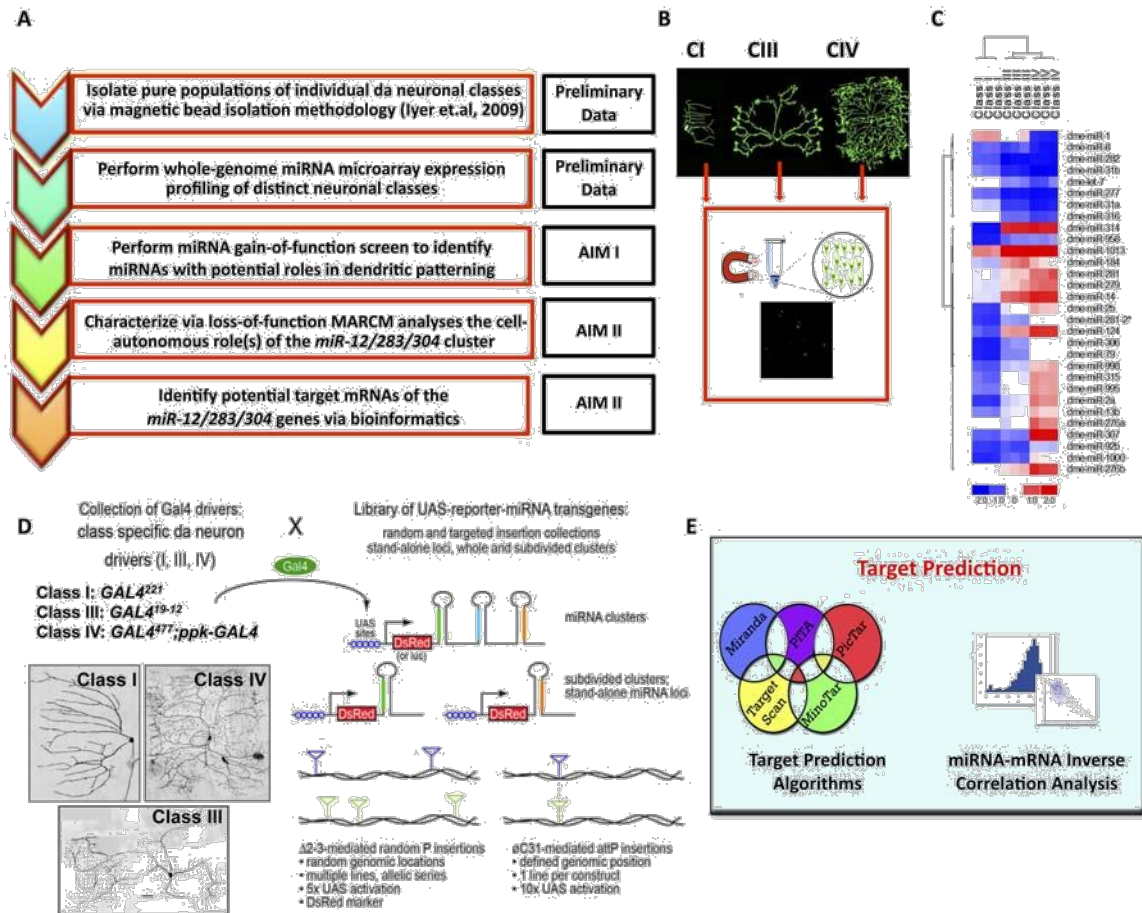


Figure 12. (A) Experimental pipeline and map of specific aims. (B) Isolation of da neuron subclasses via magnetic bead-based cell sorting. (C) Heatmap of top 30 differentially expressed miRNAs from microarray profiling. Overall 75 miRNAs were found to be significantly expressed above background in da neurons subclasses. (D) Schematic diagram of miRNome gain-of-function genetic screen. (E) Schematic diagram of target prediction algorithms and miRNA-mRNA inverse correlation analyses for bioinformatic based identification of putative target mRNAs. Panel D adapted in part from Bejarano et al. (2012).

1.12 Specific Aims:

AIM I. Explore the putative role(s) of miRNAs in mediating class-specific dendrite morphogenesis via a systematic gain-of-function genetic screen.

Hypothesis: Based on the preliminary expression matrix data and phenotypic analyses of key miRNA biogenesis machinery genes, we hypothesize that miRNAs play a critical roles in mediating class-specific dendrite morphogenesis.

Approach: We will use a targeted gain-of-function genetic screen to explore the phenotypic consequences of the miRNAs over-/mis-expression on normal da neuron dendrite development using class-specific GAL4 drivers. Phenotypic analysis will be conducted by live image, *in vivo* confocal microscopy. The resulting qualitative phenotypic analysis will be subjected to a semi-automated pipeline for digital reconstruction and quantitative analyses of dendritic morphology.

AIM II. Dissect the regulatory roles of the *miR-12/283/304* cluster in directing class-specific dendrite morphogenesis via MARCM analyses.

Hypothesis: We hypothesize, based upon preliminary phenotypic analyses, that the *miR-12/283/304* cluster of miRNAs play critical roles in regulating class-specific, morphological dendritic homeostasis.

Approach: We will conduct the loss of function (LOF) analyses, using *miR-12/283/304* null mutants and the MARCM system for generating homozygous single cell mutant clones in da

neurons in order to assess cell autonomous function. These analyses are coupled to ectopic and overexpression studies of the whole miRNA cluster and of the individual miRNAs which comprise this cluster. Phenotypic analysis will be conducted by live-image, *in vivo* confocal microscopy and compared with controls. The resulting qualitative phenotypic analysis will be subjected to a semi-automated pipeline for digital reconstruction and quantitative analyses of dendritic morphology.

1.13 Research Plan:

AIM I: Explore the putative role(s) of miRNAs in mediating class-specific dendrite morphogenesis via a systematic gain-of-function genetic screen.

For gain-of-function (GOF) studies, I will use the *GAL4/UAS* system to overexpress the gene-specific miRNA construct. These studies will hence focus on the relative effects of overexpressing miRNAs in Class I, III and IV da neurons using *GAL4²²¹,UAS-mCD8::GFP*, *GAL4¹⁹⁻¹²,UAS-mCD4-tdGFP* and *GAL4⁴⁷⁷,UAS-mCD8::GFP*; *ppk-GAL4,UAS-mCD8::GFP* reporter transgene lines, respectively (**Fig. 12D**). The library of *UAS-miR* transgenic constructs is designed to allow for the targeted expression of either individual or clusters of miRNAs and each transgene is marked with the fluorescent protein DsRed to allow for independent verification of target miR gene expression. Moreover, for each single or clustered set of miRNAs, two independent *UAS-miR* transgenes were tested to address potential position effect variegation and differential expressivity that could be observed with transgene expression. The third instar larval stage of *Drosophila* will be selected to analyze the da neuron dendritic morphology using live-imaging confocal microscopy, both in overexpression lines and wild

type as controls. Statistical analyses of dendritic morphology will be conducted by a semi-automated pipeline for digital reconstruction and quantitative analyses of dendritic morphology.

AIM II: Dissect the regulatory roles of the *miR-12/283/304* cluster in directing class-specific dendrite morphogenesis via MARCM analyses.

To dissect the regulatory role(s) of the *miR-12/283/304* cluster, I will conduct overexpression analyses of the cluster as well as the individual miRs that comprise this cluster. These phenotypic and quantitative analyses will be compared with the phenotypic effects observed upon cell-autonomous deletion of the full cluster using MARCM analyses and a null mutant of the *miR-12/283/304* cluster. To assess the cell autonomous role of *miR-12/283/304* cluster in mediating aspects of class-specific da neuron dendritic morphogenesis, I will conduct MARCM LOF analyses (**Fig. 10**) on the miRNA mutant cluster which will generate homozygous single cell mosaic clones of da neurons positively labeled by the expression of GFP. Dendritic morphology of these miRNA mutant-MARCM clones at the third instar larval stage will be analyzed by live-image confocal microscopy and compared with wild-type MARCM clones as control. Statistical analysis of dendritic morphology will then be conducted by semi-automated digital reconstruction and quantitative analyses of dendritic morphology.

CHAPTER 2: EXPERIMENTAL PROCEDURES

2.1 *Drosophila* strains and culture

The *Drosophila* strains used in these studies are as follows:

GAL4 driver stocks include: (1) *yw*; +; *GAL4*²²¹, *UAS-mCD8::GFP* (Grueber et al., 2003); (2) *w*; *GAL4*⁴⁷⁷, *UAS-mCD8::GFP/CyO-GAL80*; *ppk1.9-GAL4, UASmCD8::GFP*; (3) *GAL4*¹⁹⁻¹², *UAS-mCD4-tdGFP* (Cox lab, unpublished results).

For loss-of-function analyses, *y*, *w*, *hs-FLP*, *GAL80*, *FRT*^{19A}/*y*, *w*, *hs-FLP*, *GAL80*, *FRT*^{19A}; *80G2/80G2* stock and *FRT*^{19A} *Δ3miR/ FM7i* were used (*Δ3miR* corresponds to the null mutation for the *miR-12/283/304* cluster (Friggi-Grelín et al., 2008).

The following *UAS-RNAi* transgenic stocks were used for phenotypic validation of putative *miR-12* target mRNAs: *UAS-Syb-RNAi* (TRiP lines: HMS01678/HMS01987, corresponding to Bloomington stocks numbers B-38234/B-39067, respectively) and *UAS-Pka-C1-RNAi* (TRiP lines: JF01218/JF01188, corresponding to Bloomington stock numbers B-31277/B-31599, respectively).

For visualization of actin and microtubule cytoskeletal networks, the following classIV-specific reporter stock was utilized: *UAS-GMA*; *Gal4*⁴⁷⁷, *UAS-mCherry:Jupiter* where actin is labeled by a GFP tagged Moesin (Dutta et al., 2002; Edwards et al., 1997) and microtubules are labeled by a mCherry tagged Jupiter MAP (Chabu and Doe, 2008; McDonald et al., 2008).

Oregon-R was used as a wild-type strain (control). *Drosophila* stocks were raised on standard cornmeal-molasses-agar fly food medium

2.2 UAS-miRNA Transgenes

Two independent transgenes for each of the 75 significantly expressed miRNAs, a total of 150 miRNAs, were used for phenotypic screening (lines described in detail in Bejarano et al., 2012). Each of these UAS-DsRed-miRNA transgenes is designed to allow for the targeted expression and each transgene is marked with the fluorescent protein DsRed to allow for independent verification of target miR gene expression. The two independent *UAS-miR* transgenes were tested to address potential position effect variegation and differential expressivity that could be observed with transgene expression. For the purpose of further characterization and validation of the results by the GOF analyses of *miR-12/283/304* cluster and individuals within the cluster, we obtained 2 independent *UAS-miR-283-DsRed*, *UAS-miR-12-DsRed* and *UAS-miR-304-DsRed* transgenes.

2.3 Gain-of-function Analyses

To conduct gain-of-function analyses, a *GAL4-UAS* system was used to overexpress the UAS-DsRed-miRNA transgenes in the three class specific da neurons Class I, III and IV using class-specific drivers (1) *yw; +; GAL4²²¹,UAS-mCD8::GFP* (Grueber et al., 2003) (2) *GAL4¹⁹⁻¹²,UAS-mCD4-tdGFP* and (3) *w; GAL4⁴⁷⁷,UAS-mCD8::GFP/CyO-GAL80; ppk1.9-GAL4,UASmCD8::GFP* respectively. Specifically, the Class I da neuron driver (*GAL4²²¹,UAS-mCD8::GFP*), Class III da neuron driver *GAL4¹⁹⁻¹²,UAS-mCD4-tdGFP* and the Class IV da neuron driver (*GAL4⁴⁷⁷,UAS-mCD8::GFP/CyO-GAL80; ppk1.9-GAL4,UASmCD8::GFP*) were crossed to flies bearing the UAS-DsRed-miR transgenes resulting in transgene combinations. Studies were performed on 150 crosses of miRNA transgenes, across the three different classes of da neurons. Third instar larvae resulting from these crosses were isolated and subjected to live image confocal microscopy.

2.4 MARCM Analyses

To characterize the mutant phenotype of the miR cluster *miR-12/283/304 deletion* in da neurons, male flies of the stock *FRT^{19A} Δ3miR/ FM7i* were crossed to the virgin females of the stock *y, w, hs-FLP, GAL80, FRT^{19A}/ y, w, hs-FLP, GAL80, FRT^{19A}; 80G2/80G2* resulting in a progeny of flies with the transgene combination *y, w, hs-FLP, GAL80, FRT^{19A}/ Δ3miR FRT^{19A}; 80G2/80G2*. The null mutation is located on the X chromosome and 80G2 is a marker that is used to mark only da neurons and is present on the 2nd chromosome. Embryos were collected in an egg collection chamber for 3 hours at 25°C on a standard cornmeal media plate, incubated at 25°C for 4 hours to allow the eggs to age, then heat-shocked at 38°C for 1.5 hours and incubated at 25°C until they were analyzed as wandering third instar larvae, just prior to pupation. The incubation process at different time intervals and temperatures were performed with the help of a programmable thermocycler Echotherm Incubator. GFP-labeled clones were picked after screening the third instar larvae under a fluorescence microscope, Leica MZ F16A. The selected GFP-labeled clones representing mutant miR MARCM clone were subjected to live-image, *in vivo* confocal microscopy and compared with wild-type MARCM clones as control.

2.5 Larval preparation and live image confocal microscopy

The selected third instar larvae are collected and washed multiple times with distilled water in order to remove any excess food particles stuck to it. The cleaned larvae is then placed onto a microscopic slide and immersed in a few drops of oil consisting of anhydrous diethyl ether and halocarbon oil in the ratio 1:5, respectively. A 22 x 50 cm coverslip is placed over it and the larva is stretched out to be viewed under the confocal microscope. Qualitative phenotypic analyses of the da neurons expressing the GFP were conducted using a Nikon C1 plus confocal

microscope with the Nikon EZ-C1 software. Confocal images were collected as a series of Z-stacks at 1024 pixel resolution and a uniform step size. Z stacks were then rendered into a maximum projection and resultant images were then stitched together via Adobe PhotoshopTM CS5 for subsequent quantitative semi-automated digital reconstruction.

2.6 Semi-automated digital reconstruction and quantitative analyses of dendritic morphology

Semi-automated digital neuronal reconstruction and quantitative analyses were performed as previously described (Iyer et al., 2013). Statistical analyses such as mean, standard deviation, standard error, and two-tailed t-test were performed on the data to construct graphs using Sigma-Plot.

2.7 Bioinformatic analyses of miR cluster targets

Bioinformatic analyses of the *miR-12/283/304* miRNA cluster were performed, including target prediction and gene ontology analyses for significantly enriched biological categories of putative target genes for this cluster. Briefly, we employed the HOCTAR algorithm (<http://hoctar.tigem.it/>) (Gennarino et al., 2009, 2011) which is based upon the principle that the expression value of an intragenic miRNA can be defined by, and is tightly correlated with, the expression value of the host mRNA in which the intragenic miRNA is located. As the *miR-12/283/304* cluster is located in the fifth intron of the *Gmap* host gene, anti-correlation expression analyses were performed using *Gmap* expression as a proxy for the miR cluster. For these analyses, raw microarray data was obtained from the ArrayExpress database which contains the GEO datasets (244 experiments, each experiments containing a minimum of (5) microarray assays) (<http://www.ebi.ac.uk/arrayexpress/experiments/browse.html>) (Parkinson et al., 2007). These microarray data are normalized using the rma function of the Affymetrix

package (Gautier et al., 2004). For each experiment, microarray probe ids and expression values related to the host gene (*i.e.* *Gmap*) are obtained as proxy expression data for the *miR-12/283/304* cluster across assays from all experiments. These data are stored in the form of a hash map together with the data for all other mRNAs (probe id and expression values). Using these data, we performed both parametric (Pearson) and non-parametric (Distance) anti-correlation analyses between *Gmap* expression values and all other mRNAs using the R function `cor.test` (Pearson) and `dcor.ttest` (Distance) in order to calculate *p* values as well as correlation coefficients. These statistical comparisons are repeated across all experiments. From these analyses, a false discovery rate calculation (Benjamini Hochberg) is done on the *p* values obtained for each miRNA-mRNA pair (using the host gene as the miRNA proxy) using the `p.adjust` function in R. To identify statistically significant, anti-correlated mRNA targets for a particular miRNA, all mRNAs with a q-value of less than 0.01 are selected across all experiments. From these analyses, the top 25% most frequently occurring mRNAs are then compared with the targets predicted for a given miRNA in a variety of target databases (TargetScan, PITA, and Miranda). Target mRNAs which are in common with the target databases can then be identified and a union of the statistically significant Pearson and Distance correlation targets is retained as putative high confidence targets for a given miRNA. This list of putative target mRNAs is then uploaded to the DAVID server (<http://david.abcc.ncifcrf.gov>) (Huang et al., 2007) for functional annotation and gene ontology (GO) analyses for Biological Processes. The non-redundant functional annotations for each gene list is plotted against the enrichment values and p-values using a modified Fisher's exact test (EASE score).

CHAPTER 3: RESULTS

3.1 Functional miRNome analyses reveal complex miRNA regulation of class-specific dendrite morphogenesis.

miRNome expression profiling revealed 75 miRNAs that were enriched and/or differentially expressed above background in three independent da neuron subclasses. To investigate the putative functional roles of the miRNAs, we performed a gain-of-function genetic screen of a total of 150 transgenic lines, representing two independent lines for each single or cluster of miRNAs.

Three distinct subclasses of da neuron were investigated (Class I, III, and IV) (**Fig. 6,12**). Broadly categorized, the results of the miRNome genetic screen revealed two major phenotypic groups of genes that display miRNA-mediated regulation of dendritogenesis: (1) those miRNAs that promote and (2) those that restrict dendritic growth and branching complexity. In addition to these two major groups, a select subset of miRNA or miRNA clusters exhibited context-dependent effects on class-specific dendrite morphogenesis.

3.1.1 miRNA-mediated promotion of dendritic growth and branching

Phenotypic screen results and quantitative analyses of dendritic reconstructions from three independent da neuron subclasses (I, III, IV), identified a group of miRNAs that when over- or ectopically expressed lead to increased dendritic growth and/or branching relative to controls (**Figs. 13-15,19**). In the case of the class I neurons *ddaE* and *vpda*,

class-specific expression of this group of miRNAs led to the *de novo* formation of supernumerary dendritic branches, particularly those proximal to the cell body (**Figs. 13,19**). Of note, the other class I neuron, ddaD was not analyzed due to the fact that the class I-specific *GAL4²²¹,UAS-mCD8::GFP* reporter transgene shows weaker levels of expression in ddaD relative to equivalent levels of expression in ddaE and vpda.

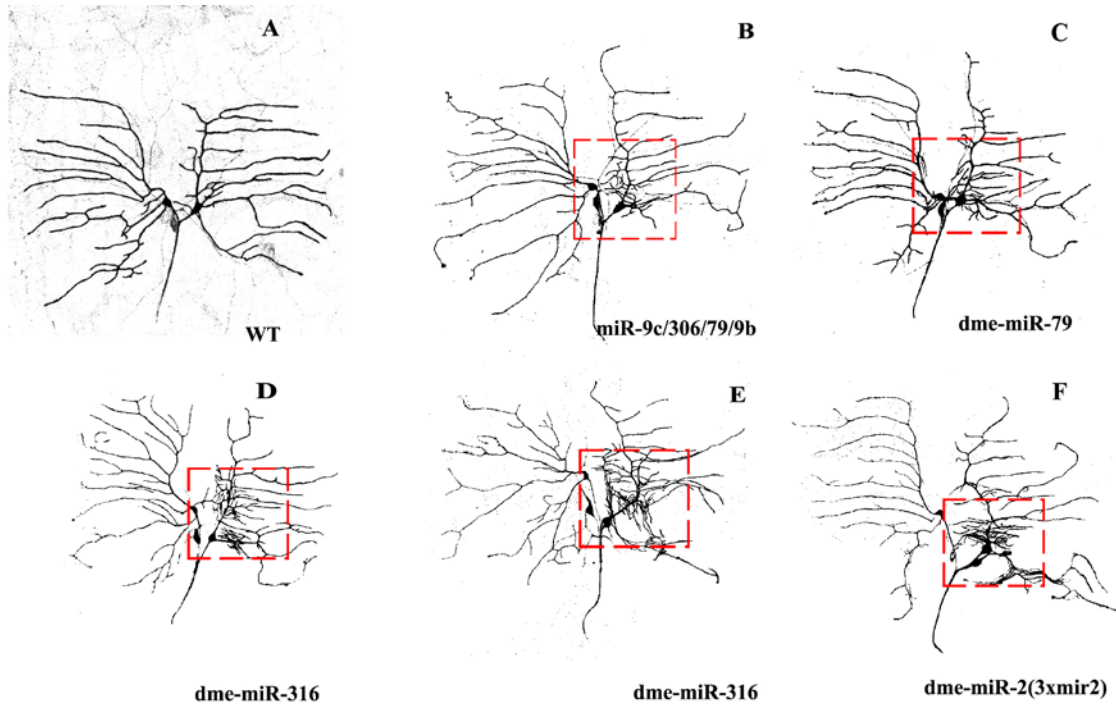


Figure 13: miR-mediated promotion of dendritic growth/branching in class I da neurons. The areas highlighted in the red dotted box above are ddaE neurons of representative miRNAs, which showed an increase in the dendritic branches and aberrant clustering pattern. **(A)** Wild-type dorsal class I neurons. **(B-F)** Representative images of over/mis-expressed miRNAs that promote class I dendrite growth/branching as measured in ddaE neurons. Note: Panels **(D)** and **(E)** are representative phenotypic examples of the same miRNA with 2 independent transgenes revealing consistent phenotypic effects of dendritic morphology.

Similarly, in class III neurons (*ddaA*; *ddaF*; *v'pda*), phenotypic analyses revealed this category of miRNAs promotes dendritic growth/branching, particularly with respect to the *de novo* formation of dendritic filopodial projections which extend from the primary and secondary dendrite branches and are a characteristic morphological feature of this da neuron subclass (**Figs. 14,19**).

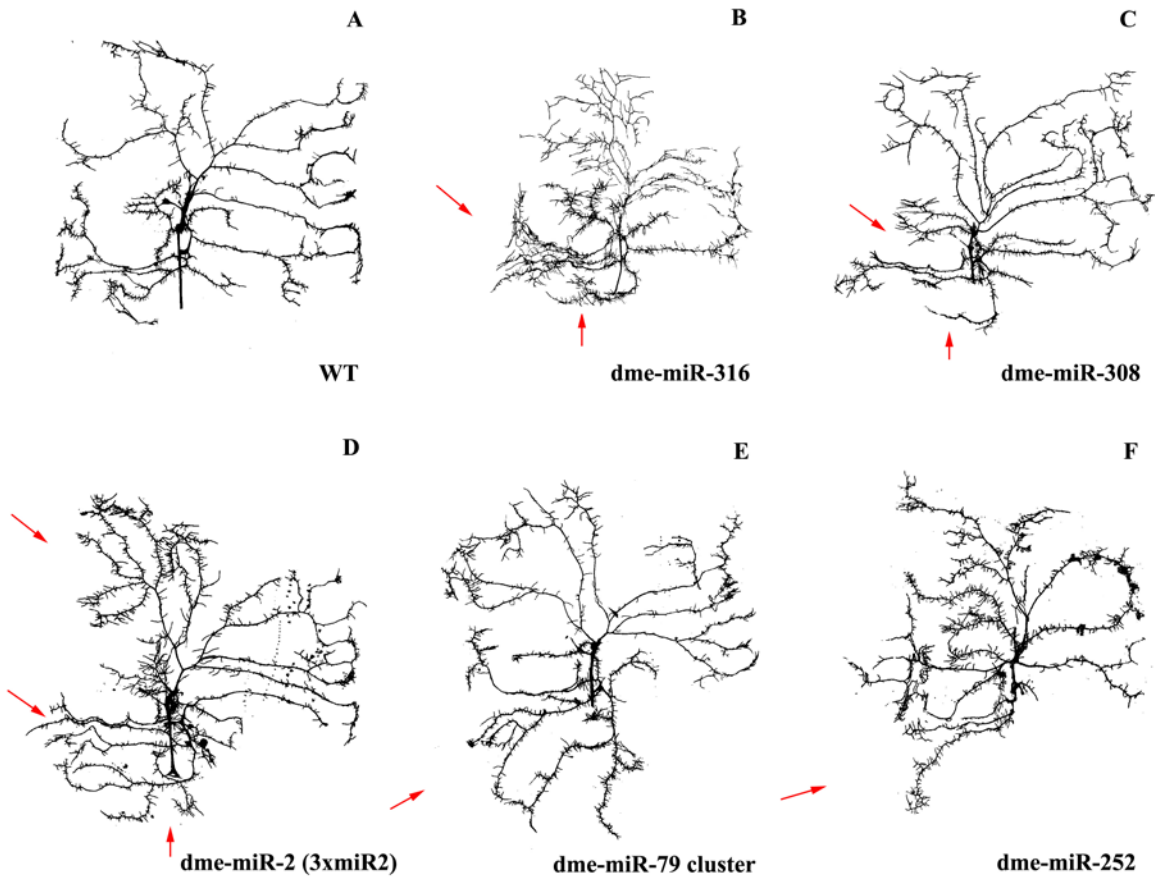


Figure 14: miR-mediated promotion of dendritic growth/branching in class III da neurons. The red arrows indicate regions where an increase of dendritic filopodial protrusions was observed in the *ddaA* and *ddaF* class III neurons. (A) Wild type dorsal class III neurons (*ddaF/A*). (B-F) Representative images of over/mis-expressed miRNAs that promote class III dendritic branching/growth as measured in *ddaA* and *ddaF* neurons.

We likewise identified a related cohort of miRNAs that exhibit differential effects on dendrite arborization relative to controls, but which quantitatively promote dendritic growth and branching in class IV da neurons (*ddaC*; *v'ada*; *vdaB*) (**Figs. 15,19**). Interestingly, miRNAs such as *dme-miR-316*, *dme-miR-79*, *dme-miR-2*, *dme-miR-9c/306/79/9b* all show a significant increase in dendritic growth and/or branching complexity across all three da neuron subclasses. Broadly considered, these data indicate that this subgroup of miRNAs likely functions by regulating the expression of genes that would otherwise limit dendritic growth and/or branching.

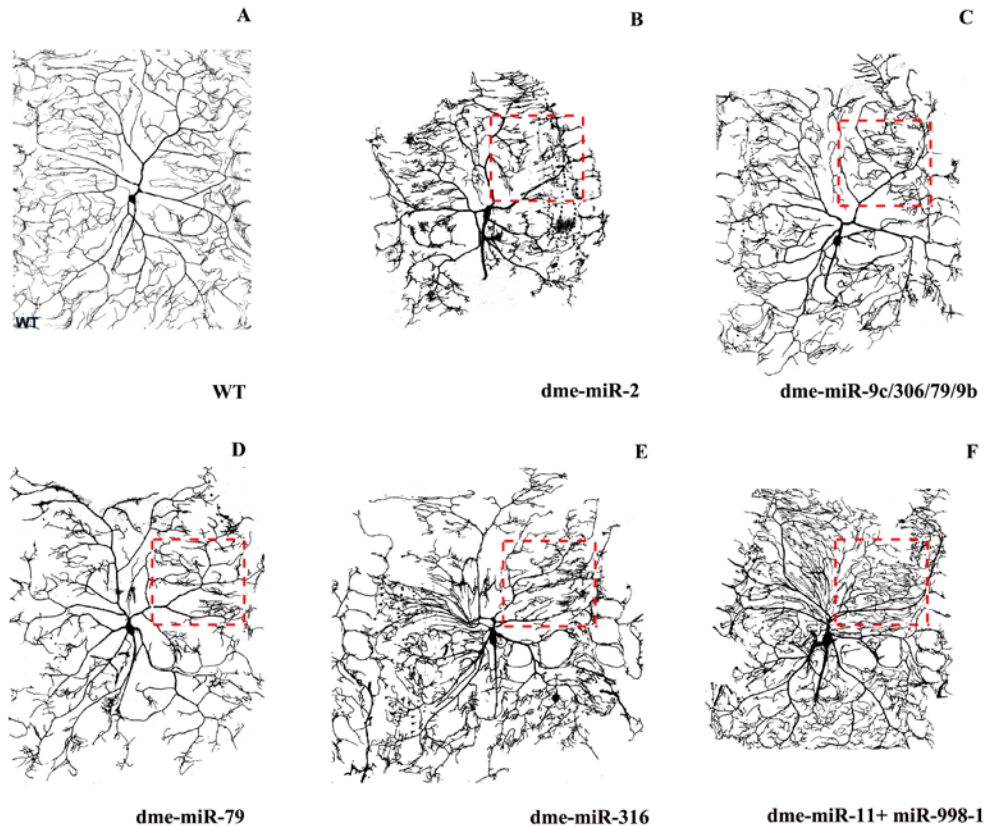


Figure 15: miR-mediated promotion of dendritic growth/branching in class IV da neurons. The red dotted box highlights increases in dendritic growth and branching observed in the class IV *ddaC* neurons. (A) Wild type dorsal class IV neuron (*ddaC*). (B-F) Representative images of over/mis-expressed miRNAs that promote class IV dendritic branching/growth as measured in *ddaC* neurons.

3.1.2 *miRNA-mediated restriction of dendritic growth and branching*

A second major phenotypic category of miRNAs identified in the screen exhibited dramatically restricted dendritic growth and branching upon over-/ectopic expression relative to controls (**Figs. 16-19**). In class I neurons, expression of this category of miRNAs produced variable effects (moderate to severe) on primary dendrite outgrowth and/or secondary lateral branching (**Figs. 16,19**). For example, over-expression *dme-miR-279* in class I neurons severely impairs secondary lateral branching and outgrowth and produces cell bodies that are qualitatively smaller in size relative to controls (**Fig. 16D**), whereas *dme-miR-34*, and *dme-miR-981* exhibit defects in primary branch specification, growth, and lateral branch formation (**Fig. 16E,F**). Consistent with previous findings (Xu et al., 2008), our analyses also revealed significant reductions in dendritic branching for the nervous-system specific *dme-miR-124* (**Fig. 16C**). Similarly, miRNAs in this category showed strong reductions in dendritic growth and/or branching in both class III (**Figs. 17,19**) and IV da neurons (**Figs. 18-19**). In class III neurons, expression of many of these miRNAs restricts or inhibits the formation of dendritic filopodia producing a largely stripped dendritic architecture. For example, overexpression of the *miR-263a* (**Fig. 17D**) and *miR-34* (**Fig. 17F**) nearly inhibits the formation of filopodia, whereas overexpression of *miR-124* (**Fig. 17E**) has a greater phenotypic effect on restricting dendritic growth and field coverage. With respect to class IV neuron dendrite morphogenesis, overexpression of miRNAs in this category likewise produced differential effects on dendritic growth, branching and field coverage, albeit in the case of these miRNAs the effects led to overall reductions in dendrite development (**Figs. 18-19**). Overexpression of the *miR-100/125/let7* cluster (**Fig. 18C**)

and *miR-279* (**Fig. 18F**) in class IV ddaC neurons resulted in rudimentary dendritic growth, disruptions in higher order branching and reduced field coverage relative to controls, whereas overexpression of *miR-277* (**Fig. 18D**) and *miR-1* (**Fig. 18E**) led to a shift in dendritic branching architecture characterized by distal terminal tufting and increased formation of short, filopodial-like dendritic extensions from the primary and secondary branches. Collectively, these data indicate that this subgroup of miRNAs likely functions by regulating the expression of genes that would otherwise promote dendritic growth and/or branching.

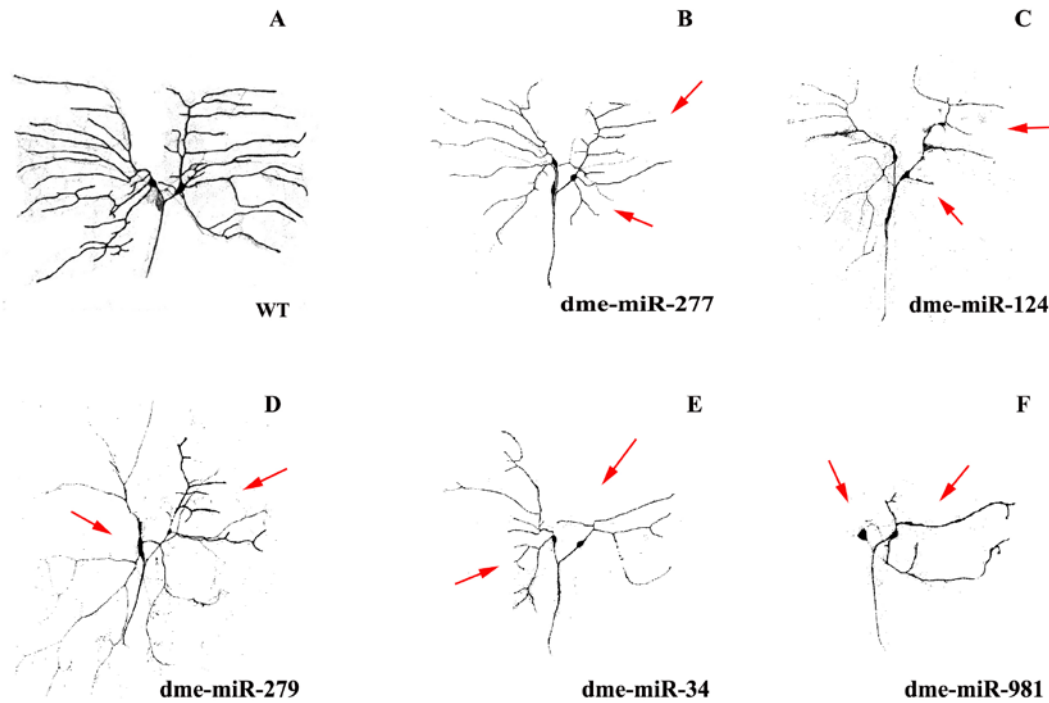


Figure 16: miR-mediated repression of dendritic growth/branching in class I da neurons. The red arrows indicate the reductions observed in ddaD and ddaE neurons. (A) Wild-type dorsal class I neurons. (B-F) Representative images of over/mis-expressed miRNAs that repress class I dendrite growth/branching.

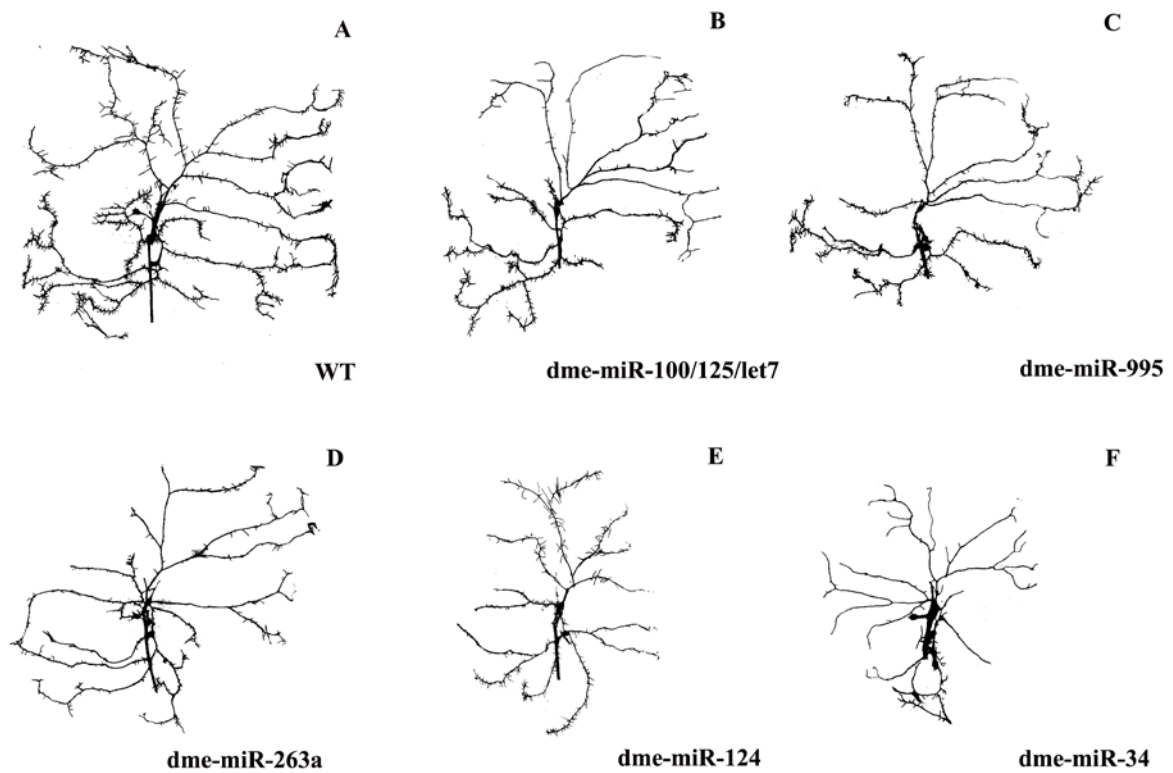


Figure 17: miR-mediated repression of dendritic growth/branching in class III *da* neurons. (A) Wild type dorsal class III neurons (*ddaF/A*). (B-F) Representative images of over/mis-expressed miRNAs that repress class III dendritic branching/growth and filopodia formation as measured in *ddaA* and *ddaF* neurons.

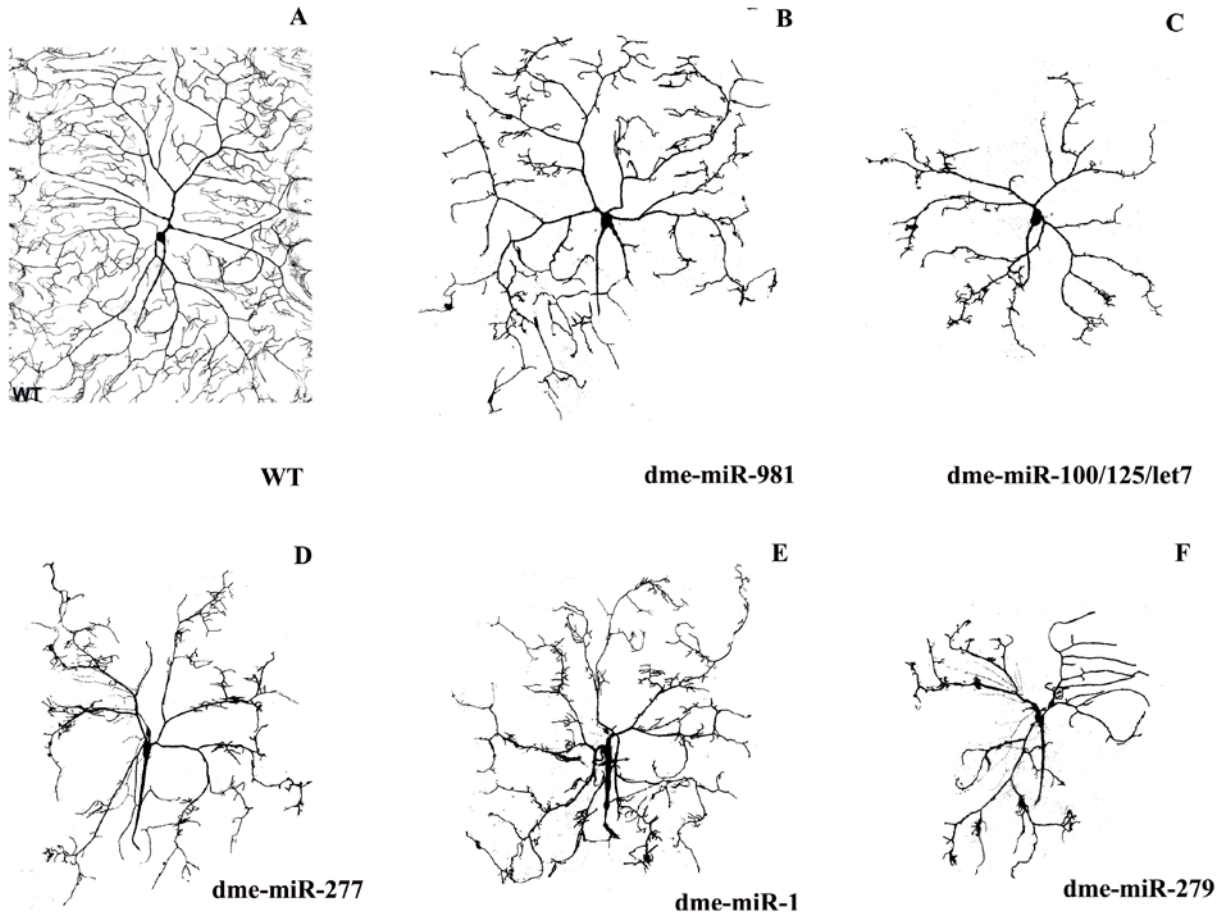


Figure 18: miR-mediated repression of dendritic growth/branching in class IV *da* neurons. (A) Wild type dorsal class IV neuron (ddaC). (B-F) Representative images of over/mis-expressed miRNAs that reduce class IV dendritic branching/growth as measured in ddaC neurons.

3.1.3 *Quantitative analyses of miRNA-mediated dendrite morphogenesis*

For all of the above phenotypic studies, we performed quantitative analyses by digitally reconstructing the dendritic morphology from miR overexpression lines and compared this data to wild-type controls for each class of da neuron. The quantitative neuromorphometric analyses of dendrite morphology revealed that a broad spectrum of significantly expressed miRNAs result in statistically significant effects on the number of dendritic branches and total dendritic length relative to controls (**Fig. 19**). In total, we performed ~12,000 digital reconstructions for our quantitative analyses of the miRNome dendritic morphogenesis screen (**Fig. 20**).

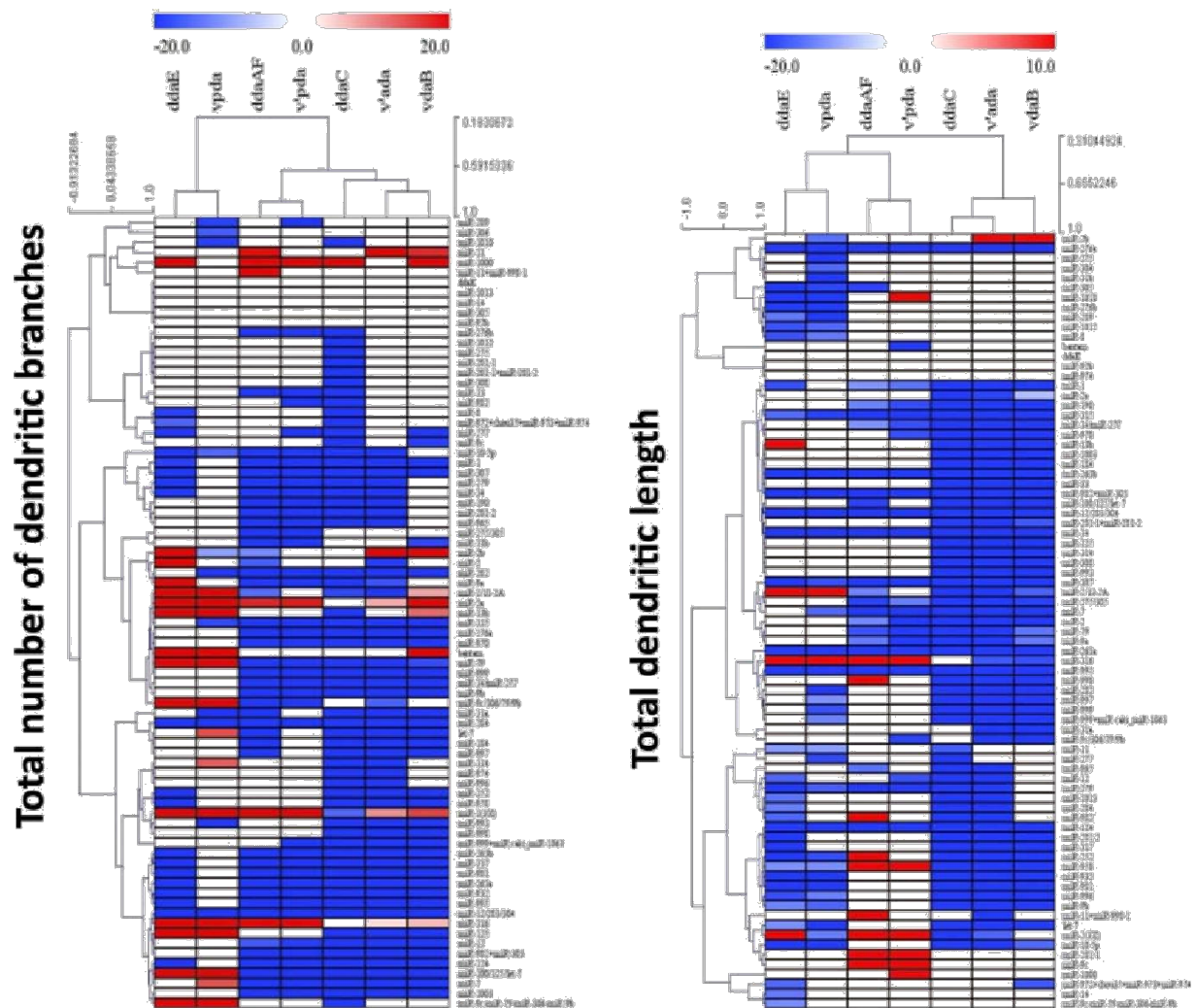


Fig. 19: Quantitative analyses of dendritic morphologies. Average % change from control for a given quantitative neurometric parameter is represented for each miRNA as a heatmap with colored gradients, where varying intensities of red represents increases, blue represents decreases and white represents no change. All data represent statistically significant ($p < 0.05$) changes relative to wild-type controls.

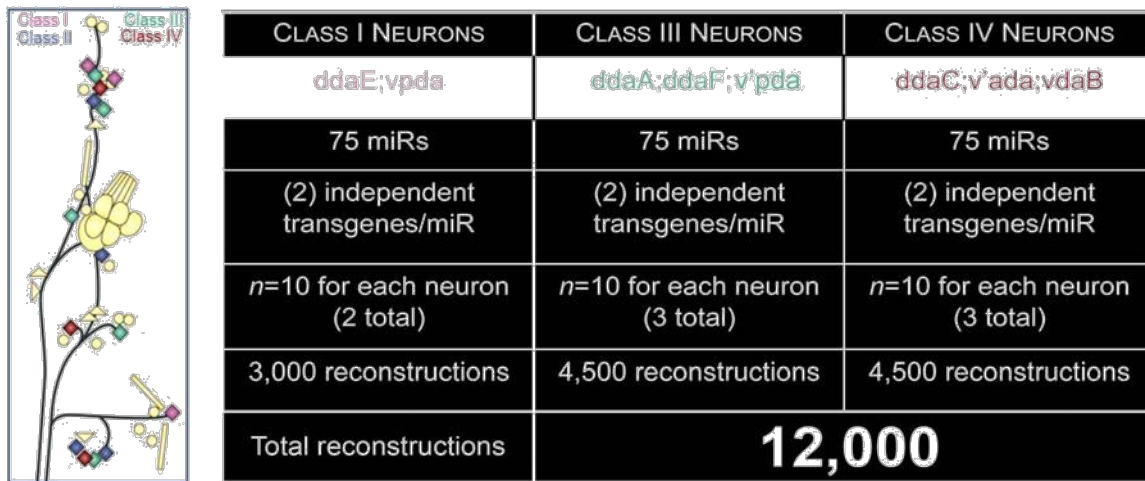


Fig. 20: Summary of neuromorphometric digital reconstructions of da neurons by class for the miRNome genetic screen. Shown at left is a schematic of the distribution of individual da neuron subclasses within a larval abdominal hemisegment.

3.2 The miR-12/283/304 cluster functions in fine-tuning class-specific dendritic diversity

Results of our systematic phenotypic screens provide the first large-scale analyses of the biological activities of miRNAs in regulating class-specific dendritic architecture. Given that our analyses were based upon those miRNAs that were significantly enriched and/or differentially expressed in da neuron subclasses, it is certainly likely that the phenotypic effects observed are due to over-expression or ectopic expression of the individual or cluster of miRNAs. Nevertheless, these *in vivo* gain-of-function analyses enable a global phenotypic profile of the consequence of miRNA deregulation, as well as potentially providing instructive insight into the possible native functional roles for these genes in dendrite morphogenesis. Consistent with this, previous studies have revealed the power of such gain-of-function genetic screens in identifying and characterizing biological processes of interest, including miRNA function and dendrite development (Abdelilah-Seyfried et al., 2000; Ou et al., 2008; Kraut et al., 2001; Bejarano et al.,

2012). To assess the biological significance of these deregulated miRNA phenotypes, it is important to examine whether these gain-of-function effects are relevant to native endogenous gene function.

To directly address this question, we elected to analyze a particular intronic miRNA cluster, composed of *miR-12*, *miR-283* and *miR-304* (*miR-12/283/304* cluster) via both mutant and overexpression phenotypic analyses. The *miR-12/283/304* cluster is an intragenic miRNA cluster that maps within the fifth intronic sequence of *dGMAP* on the X chromosome (Friggi-Grelín et al., 2008). Our miRNA expression profiling analyses revealed that components of this cluster, specifically *miR-12* and *miR-304*, exhibit significant expression above background, and differential expression among da neuron subclasses. Consistent with this observation, previous studies revealed that the *miR-12/283/304* cluster is embryonically expressed in a subset of PNS sensory neurons (Aboobaker et al., 2005). Specifically, we find that *miR-12* and *miR-304* are significantly enriched in morphologically complex class III and IV da neurons relative to the simpler class I neurons (**Fig. 21A**). Moreover, we observed higher levels of *miR-12* expression relative to *miR-304* in class III/IV da neuron subtypes, with the highest expression levels in class III neurons, followed by slightly lower levels in class IV neurons. While *miR-283* was also detected in the miRNA expression arrays, the probe intensity was less than 1.5X of the signal intensity for whole larvae controls indicating that while expressed, *miR-283* is not significantly enriched in these da neuron subclasses relative to background. Despite this fact, previous studies have demonstrated that components of miRNA clusters commonly exhibit coordinate gene expression (Wang et al., 2011) and

previous reports have revealed co-expression of these three miRNAs (*12/283/304*) (Friggi-Grelín et al., 2008; Leaman et al., 2005). The differential expression observed for *miR-12* and *miR-304* suggested that this miRNA cluster might function in regulating class-specific dendritic diversity. Moreover, it is interesting to note that these three mature miRNAs display similar sequence relationships with one another indicating potentially overlapping targets among these miRNAs (**Fig. 21B**). Consistent with this, *miR-12* and *miR-283* share homology with human *hsa-miR-496*, while *miR-304* shares the greatest homology with human *hsa-miR-216a* (Ibanez-Ventoso et al., 2008).

To test endogenous gene function, we performed MARCM analyses using a null mutation that deletes the miRNA cluster (Friggi-Grelín et al., 2008). Given the higher expression levels for members of the cluster in class III and IV da neurons (**Fig. 21A**), we focused our initial MARCM studies on these neuron subclasses. In both subclasses, miR cluster deletion produced cell autonomous defects in dendritic branching and growth (**Fig. 21C-J**). Relative to control neurons, the primary phenotypic defect observed in class III neurons was a strong reduction in the formation of actin-rich dendritic filopodia, which are distinguishing morphological features this da neuron subclass (**Fig. 21C,D**). This observation is supported by quantitative neuromorphometric analyses that reveal significant reductions in both dendritic branching and growth (**Fig. 21G,H**). Similarly, in class IV neurons, while the primary dendritic branches are relatively unaffected, cluster deletion produced significant phenotypic defects in dendritic growth and branching (**Fig. 21I,J**) resulting in reductions in higher order branching and field coverage, relative to controls (**Fig. 21E,F**). To determine if these phenotypic effects are observed in other da

neuron subclasses, we extended our MARCM studies to include class I and II neurons. These analyses revealed a significant reduction in dendritic growth for both class I and II neurons (**Fig. 22A-D,F,H**) relative to controls, however a significant reduction in higher order dendritic branching was only observed in class II neurons (**Fig. 22C,D,G**). Collectively, these mutant studies implicate the *miR-12/283/304* cluster is cell autonomously regulating higher order dendritic branching, including the formation of actin-rich dendritic filopodia, as well as dendritic growth, among da neuron subclasses.

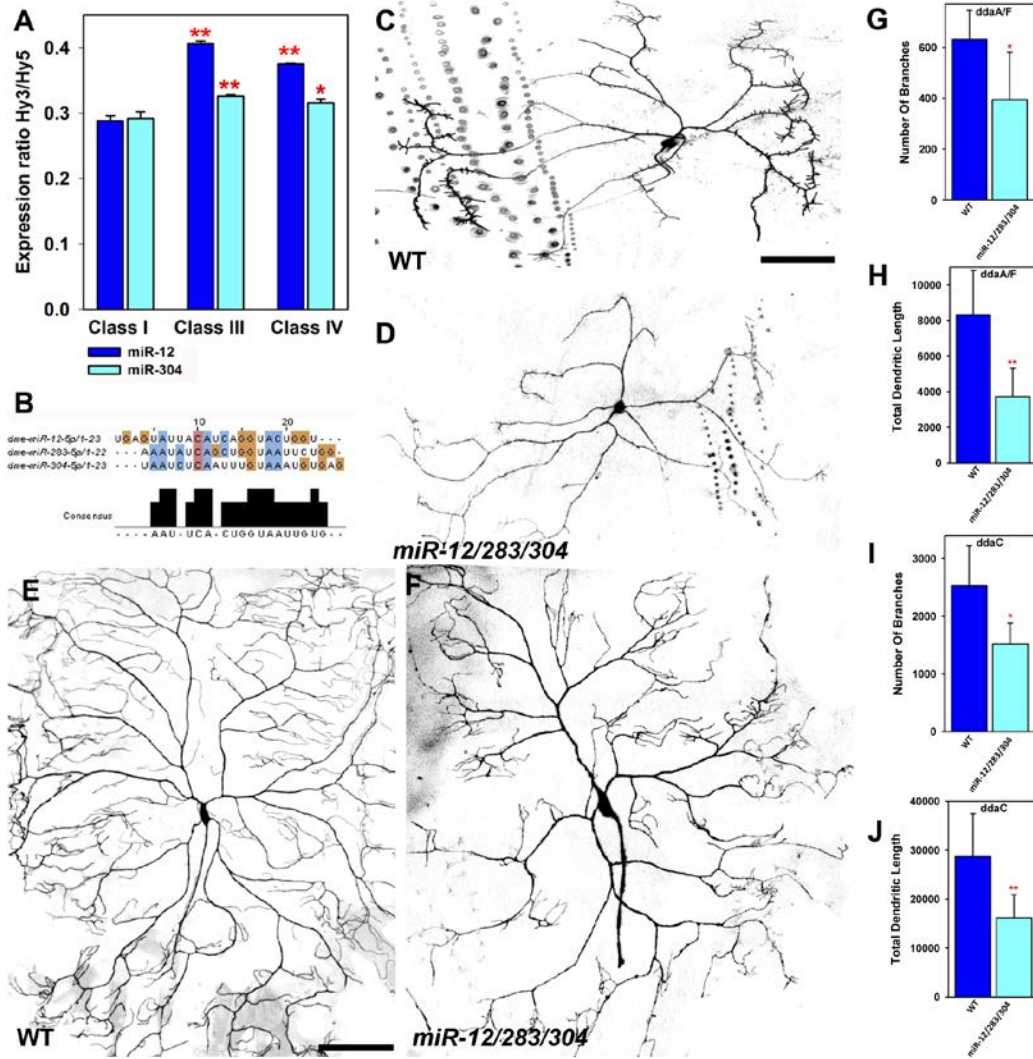


Figure 21: MARCM analyses implicate the *miR-12/283/304* cluster in cell autonomously regulating higher order dendritic branching and overall growth in class III and IV da neurons. (A) Class-specific miRNA profiling expression ratios (Hy3/Hy5 signal; mean±SEM, $n=3$) reveal significant enrichment above whole larval controls for *miR-12* and *miR-304* in class I, III, and IV da neurons. Comparative quantitative analyses indicate differential expression of these miRNAs with significantly higher levels in class III/IV neurons relative to class I. (B) Sequence relationships of miRNA cluster genes (*miR-12/283/304*) with consensus sequence indicated below the alignments. (C-F) Representative wild-type (WT) (C,E) and *miR-12/283/304* mutant (D,F) third instar larval MARCM clones. (C,D) Class III ddaA clones; (E,F) class IV ddaC clones. Scale bars correspond to 100 microns. (G-J) Quantitative neurometric analyses of the number of dendritic branches (G,I) and total dendritic length (μm) (H,J) for class III (ddaA/F) and IV (ddaC) neurons, respectively. Due to low clonal frequency, for class III neurons, equivalent numbers of wild-type and mutant ddaA and ddaF neurons were compared. Neurometric data ($n=5-6$ neurons/genotype) is expressed as mean±s.d. (G-J) and pairwise comparisons were performed by a Student's *t*-test relative to controls (*) $p \leq 0.05$; (**) $p \leq 0.01$.

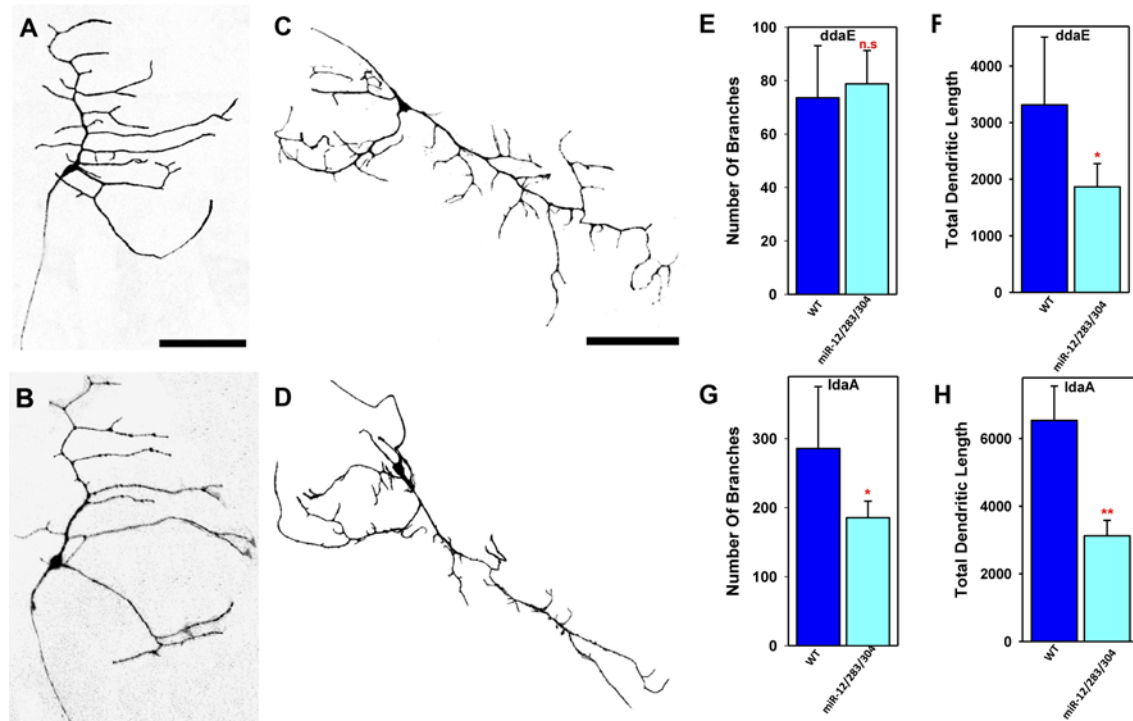


Figure 22: MARCM analyses reveal differential roles for the *miR-12/283/304* cluster in mediating higher order dendritic branching and growth in class I and II da neurons. (A-D) Representative wild-type (WT) (A,C) and *miR-12/283/304* mutant (B,D) third instar larval MARCM clones. (A,B) Class I *ddaE* clones; (C,D) class II *IdaA* clones. Scale bars correspond to 100 microns. (E-H) Quantitative neurometric analyses of the number of dendritic branches (E,G) and total dendritic length (μm) (F,H) for class I and II neurons, respectively. Neurometric data ($n=5$ neurons/genotype) is expressed as mean \pm s.d. and pairwise comparisons were performed by a Student's *t*-test relative to controls (*) $p\leq 0.05$; (**) $p\leq 0.01$.

3.3 Overexpression analyses reveal distinct functional roles of miRNA cluster components

Although individual miRNA mutants for components of this cluster do not exist, we reasoned that complementary overexpression phenotypic analyses could be used to further dissect the individual contributions of the cluster miRNAs to regulating dendrite development. For these analyses, we focused on class III and IV da neurons which displayed the highest levels of expression for cluster components and conducted overexpression studies of each individual miRNA, as well as the full cluster. In each

case, a minimum of two independent *UAS* transgenes were used for single and clustered miRNAs to control for potential transgene position effects. Moreover, multiple class III (ddaA/ddaF/v'pda) and class IV (ddaC/vdaB) neurons were analyzed to assess any subtype-specific phenotypic effects (**Figs. 23,24**). Relative to controls, overexpression of *miR-12* produced a dramatic increase in the formation of dendritic filopodia in class III neurons, consistent with the mutant effects observed with full cluster depletion (**Fig. 23B**). In support of this observation, neurometric analyses revealed that *miR-12* overexpression leads to a significant increase in overall branch density (total number of branches/total dendritic length) (**Fig. 23F**), whereas the average branch length was significantly reduced (**Fig. 23G**). These data indicate that *miR-12* expression promotes the *de novo* formation of short dendritic filopodia. With respect to *miR-304*, overexpression produced a similar phenotypic trend to that observed for *miR-12* in class III neurons (**Fig. 23C**), albeit to a lesser extent. *miR-304* overexpression leads to a mild, but significant, increase in branch density (**Fig. 23F**) with a concomitant reduction in average branch length among selected class III neurons (ddaA/F) (**Fig. 23G**). In contrast, *miR-283* overexpression leads to the opposite phenotypic trend from the other two cluster components resulting in reduced dendritic branch formation and overall growth (**Fig. 23D**). These phenotypic data are corroborated by significant reductions in branch density (**Fig. 23F**), and increases in average branch length, relative to controls (**Fig. 23G**). Interestingly, full cluster overexpression resulted in an intermediate composite phenotype that lies between the *miR-12/304* vs. *miR-283* effects (**Fig. 23E**). Quantitative analyses reveal significant reductions in branch density for v'pda neurons (**Fig. 23F**). In addition, analyses of average branch length revealed a mixed effect whereby a mild reduction was

observed in one of two overexpression lines for the *ddaA/F* neurons and a mild increase in one of two lines for *v'pda* (**Fig. 23G**). These data, together with the individual miRNA overexpression results, suggest that *miR-12*, and to a lesser extent *miR-304*, act in a similar direction to promote dendritic growth and branching, especially actin-rich filopodia, whereas *miR-283* acts to restrict these processes such that with full cluster overexpression there is an intermediate phenotype reflective of the opposing functional roles of these miRNAs in mediating class III dendrite morphogenesis.

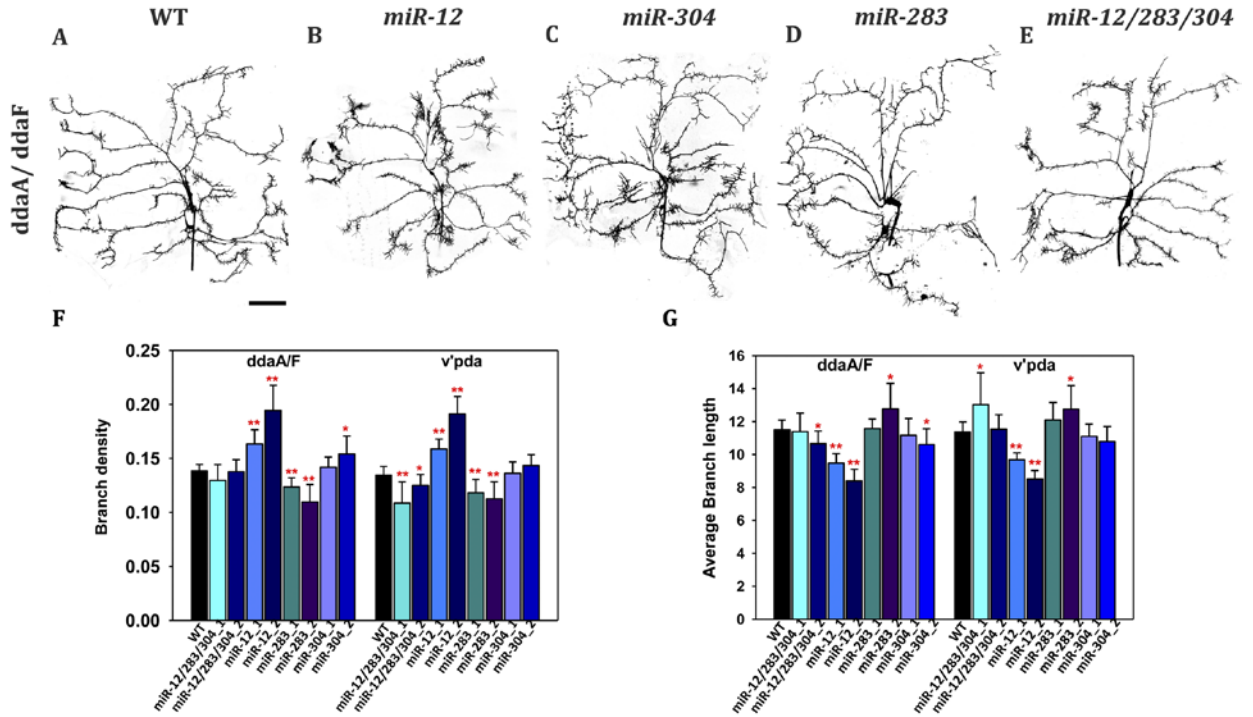


Figure 23: Overexpression analyses reveal differential and opposing roles for miR cluster components. (A) Wild type dorsal class III neurons (*ddaA/F*). (B-E) Representative images of *miR-12* (B), *miR-304* (C), *miR-283* (D), and *miR-12/283/304* cluster (E) overexpression in class III neurons via *GAL4¹⁹⁻¹²,UAS-mCD8::GFP*. Scale bars correspond to 100 microns. Quantitative neurometric analyses of branch density (F) and average branch length (μm) (G) for class III *ddaA/F* and *v'pda* neurons. In all cases, two independent *UAS-miRNA* lines were used. Neurometric data ($n=8$ neurons/genotype) is expressed as mean \pm s.d. and pairwise comparisons were performed by a Student's *t*-test relative to controls (*) $p\leq 0.05$; (**) $p\leq 0.01$.

Expression profiling revealed that *miR-12* and *miR-304* are more highly enriched in class III neurons relative to class IV, so to further dissect the functional roles of these miRNAs in class-specific dendrite development, we conducted overexpression analyses in class IV neurons. Intriguingly, these studies revealed that overexpression of cluster components produced consistent phenotypic effects, in class IV neurons, to the effects observed with class III and, moreover, that overexpression of specific cluster miRNAs alter the characteristics of class IV dendrites to acquire dendritic properties normally observed only in class III neurons (filopodia) (**Fig. 24**). Specifically, both *miR-12* and *miR-304* overexpression promote the formation of short dendritic filopodia in class IV neurons (**Fig. 24B,C**), similar to effects observed with overexpression of these miRNAs in class III neurons. Consistent with this phenotype, *miR-12* and *miR-304* overexpression results in an increase in branch density (**Fig. 24F**) and a reduction in average branch length (**Fig. 24G**), relative to controls. In contrast, *miR-283* overexpression leads to the opposite phenotypic trend with reductions in branch density (**Fig. 24D,F**) for vdaB neurons and increases in average branch length for all class IV neurons analyzed (**Fig. 24G**). These findings are consistent with the regulatory relationships observed for these miRNAs in class III neurons. Cluster overexpression in class IV neurons leads to a phenotype similar to that observed with *miR-12* overexpression whereby class IV neurons exhibit an increased incidence of filopodial extensions and a reduction in overall growth (**Fig. 24E**). Quantitatively, we find that cluster overexpression leads to an increase in branch density (**Fig. 24F**) and a reduction in average branch length (**Fig. 24G**). While these quantitative measures only achieved significance in vdaB neurons, ddaC neurons show a similar phenotypic trend. Collectively, these data indicate that regulated expression of members

of this miRNA cluster is important for promoting class-specific dendritic diversity and arborization characteristics.

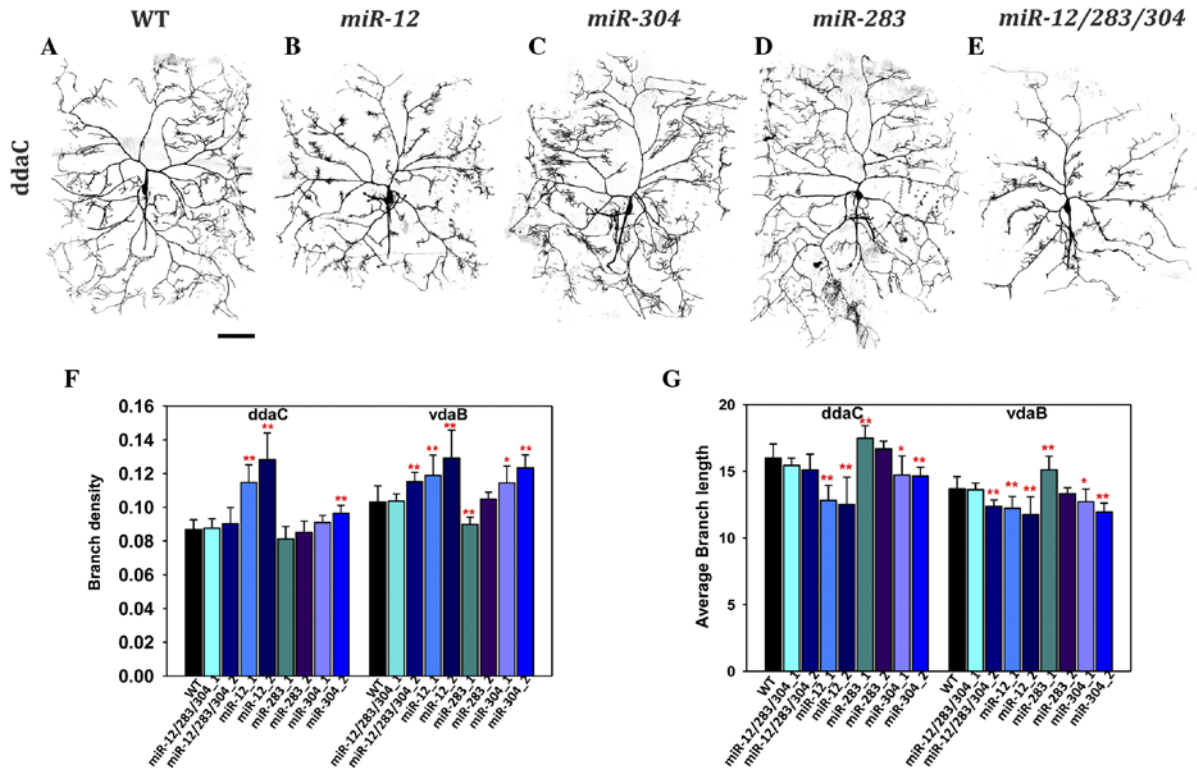


Figure 24: Overexpression analyses strongly implicate *miR-12* in promoting class-specific dendritic diversity. (A) Wild type dorsal class IV neuron (ddaC). (B-E) Representative images of *miR-12* (B), *miR-304* (C), *miR-283* (D), and *miR-12/283/304* cluster (E) overexpression in class IV neurons via *GAL4⁴⁷⁷,UAS-mCD8::GFP; ppk1.9-GAL4,UAS-mCD8::GFP*. Scale bars correspond to 100 microns. Quantitative neurometric analyses of branch density (F) and average branch length (μm) (G) for class IV ddaC and vdaB neurons. In all cases, two independent *UAS-miRNA* lines were used. Neurometric data ($n=7-9$ neurons/genotype) is expressed as mean±s.d. and pairwise comparisons were performed by a Student's *t*-test relative to controls (*) $p \leq 0.05$; (**) $p \leq 0.01$.

These data argue that *miR-12* expression correlates with the development of dendritic filopodia that are characteristic of class III neurons and not normally present in class IV neurons and that *miR-12* overexpression in class IV neurons alters class-specific dendritogenesis towards a class III morphology. Interestingly, comparative analyses of

control class III/IV neurons and *miR-12* overexpressing class IV neurons reveal a quantitative trend with respect to branch density and average branch length which are indicative of a shift towards neurometric properties characteristic of wild-type class III neurons (**Table 1**).

Genotype	Avg. Branch Density	Avg. Branch Length
Control class IV (ddaC/vdaB)	0.095	14.85 microns
<i>miR-12</i> OE class IV (ddaC/vdaB)	0.123	12.32 microns
Control class III (ddaA/F/v'pda)	0.136	11.43 microns

Table 1: Comparative neurometric analyses implicate *miR-12* in promoting dendritic diversity and regulation of class III-specific arborization characteristics. Comparative quantitative neurometric analyses reveal that *miR-12* overexpression (OE) in class IV da neurons shifts the dendritic morphology properties of these neurons towards those characteristic of class III neurons with respect to average branch density and average branch length. Data reported in table represent the average values obtained for each genotype across multiple class III and IV da neurons. For control class IV, $n=16$; control class III, $n=16$; *miR-12* OE class IV, $n=28$ (includes data from both *UAS-miRNA* transgenes).

To further examine how *miR-12*, and the other cluster components, may molecularly regulate class-specific dendritogenesis, we performed anti-correlation bioinformatic analyses of putative targets for these miRNAs (see Materials and Methods). Gene ontology (GO) analyses for anti-correlated target genes revealed a number of highly relevant and significantly enriched biological categories and cellular processes, including neuron differentiation/development, cell morphogenesis, and actin cytoskeleton organization (**Fig. 25A**). Among the list of highly anti-correlated target genes from our bioinformatic analyses, we selected two top ranking genes, *Pka-C1* and *Syb*, to investigate as potential functional targets of *miR-12*. Given that *miR-12* overexpression in class IV neurons leads to a phenotypic shift towards a class III-like morphology, we

reasoned that knockdown of putative target genes for this miRNA may likewise produce phenotypic changes that promote the formation of dendritic filopodia in these neurons. In fact, *Pka-C1* and *Syb* are putative targets of both *miR-12* and *miR-283* and consistent with our hypothesis, RNAi-mediated knockdown of these target genes in class IV neurons leads to a qualitative increase in the formation of dendritic filopodia consistent with the *miR-12* overexpression phenotype (**Fig. 25B**). To directly confirm that *miR-12* mediates the formation of these actin-rich filopodia, we analyzed actin and microtubule cytoskeletal organization in *miR-12* overexpressing class IV neurons relative to controls. These analyses demonstrate that the induced dendritic filopodia are actin-rich processes and that the primary defects observed with *miR-12* overexpression are due in large part to reorganization of the actin-based cytoskeleton (**Fig. 25C,D**). These findings are consistent with the target GO analyses that implicate members of this miRNA cluster in regulating actin cytoskeletal organization (**Fig. 25A**).

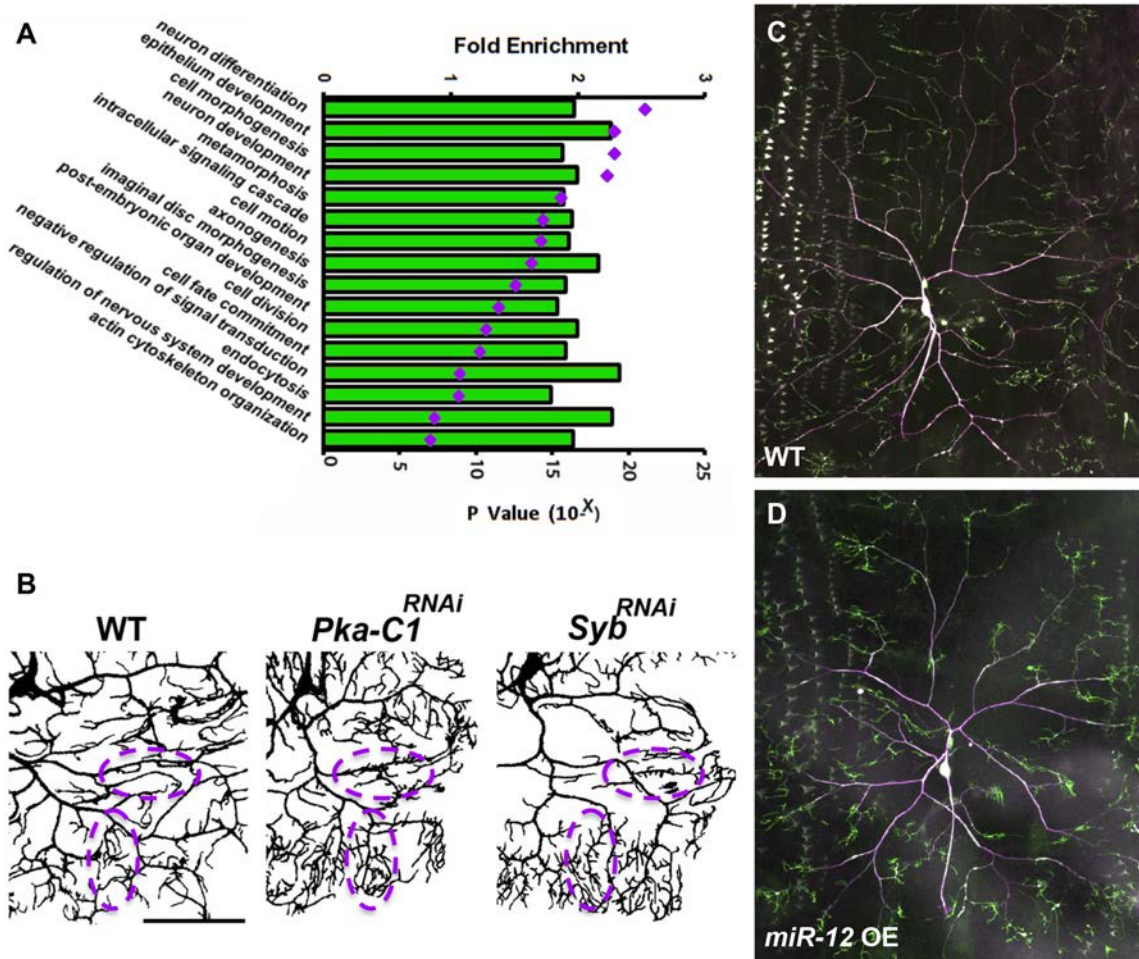


Figure 25: *miR-12* mediated regulation of dendritic arborization. (A) Gene ontology fold enrichment analyses of biological categories for putative target genes which exhibit anti-correlated gene expression patterns for the *miR-12/283/304* cluster. Diamonds indicate the modified Fisher's exact p-value for each biological category. (B) Class IV vdaB neurons labeled by *GAL4⁴⁷⁷,UAS-mCD8::GFP;ppk1.9-GAL4,UAS-mCD8::GFP*. Relative to wild-type controls (WT), RNAi knockdown of the putative *miR-12* target mRNAs *Pka-C1* and *Syb* leads to increased formation of short dendritic filopodia (compare regions highlighted by dashed magenta circles). Size bar corresponds to 100 microns. (C,D) Organization and distribution of actin (green) and microtubule (magenta) based cytoskeletons in WT (C) and *miR-12* overexpressing (D) class IV ddaC neurons. In *miR-12* overexpressing (OE) neurons there is a reorganization of actin cytoskeleton leading to the *de novo* formation of actin-based dendritic filopodia. Dendritic actin and microtubule cytoskeletons are visualized by *GAL4⁴⁷⁷*-mediated expression of *UAS-GMA* (green, actin) and *UAS-mCherry::Jupiter* (pseudo-colored magenta, microtubules).

Taken together, these studies reveal that the *miR-12/283/304* gene cluster acts in fine-tuning class specific dendritic diversity and suggest that *miR-12* plays a particularly important role in regulating the development of actin-rich dendritic filopodia which represent a defining morphological feature of this neuronal subtype. Moreover, these studies provide direct proof of principle that overexpression analyses can be instructive in deciphering the endogenous functional roles for miRNAs and can be beneficial in dissecting individual requirements of miRNAs that normally exist in a cluster and exhibit coordinate gene expression.

CHAPTER 4: DISCUSSION

4.1 miRNome analyses reveal complex functional roles for miRNAs in mediating class-specific dendritic development

Collectively, the results obtained from the gain-of-function miRNA studies revealed two major categories of regulatory effects: (1) those miRs that promote dendritic branching and growth; and (2) those miRs that restrict dendritic branching and growth. As miRNAs have been demonstrated to “fine-tune” gene expression in distinct cell types, it is consistent that on a continuum of morphological complexity from class I to IV da neurons that there would be differential expression of these two major categories of miRNAs which converge to regulate target gene expression that contributes to class-specific dendrite arborization patterns and morphological homeostasis.

For example, our data indicate that selected miRNAs mediate the promotion of dendritic branching complexity, such as *miR-12*, *miR-316*, *miR-9c/306/79/9b*, which indicates that these miRNAs normally function to repress the expression of target genes that limit dendritic branching/growth. In contrast, miRNAs involved in mediating the repression of dendritic branching complexity/growth, such as *miR-124*, *miR-12/283/304*, *miR-279*, *miR-34*, and *miR-100/125/let7*, function in repressing the expression of target genes that promote dendritic branching complexity/growth.

The results of this gain-of-function genetic screen provide the first global evidence for the regulatory roles miRNAs play in directing cell-type specific dendritic architecture. Future studies will focus on loss-of-function and target gene analyses via

which miRNA regulatory networks govern this process, as well as neural circuit formation and sensory behaviors, including nociception, at the mechanistic level.

Moreover, as a very high percentage of the miRNAs identified in our expression profiling and genetic screens are evolutionarily conserved in vertebrates (Ibáñez-Ventoso et al., 2008), our functional studies dramatically extend our understanding of the roles of miRNAs in driving dendrite development which is an essential process in the establishment, maintenance, and modulation of a functional nervous system and has well-documented neuro-anatomical correlates with neurological, cognitive, and neurodegenerative disease state pathologies.

In addition, we have implemented an integrative bioinformatic analysis platform involving inverse correlation analyses between miRNA and mRNA expression profiling data in combination with pre-existing target prediction algorithms (**Fig. 12E**) for identification of candidate mRNA targets for a given miRNA. Such inverse correlation bioinformatics-based approaches will also be employed in future in identifying high confidence, statistically significant candidate mRNAs that mechanistically regulate the production of differential dendritic architectures.

4.2 Functional analyses of the *miR-12/283/304* miRNA cluster

These analyses reveal that miRs play a critical role in regulating dendritic architectural diversity. For example, our analyses of the *miR-12/283/304* gene cluster highlights the complex regulatory effects by which miRs fine tune class specific dendritic diversity. Expression studies indicate that *miR-12* and *miR-304* are differentially enriched in complex class III and IV da neurons relative to the morphologically simpler

class I neurons. MARCM mutant studies on null mutants for this cluster indicate that these miRs contribute to cell autonomously regulating higher order dendritic branching, particularly the formation of actin-rich dendritic filopodia, as well as in promoting overall dendritic growth. Moreover, our overexpression analyses not only revealed individual regulatory effects on dendritogenesis for this cluster, but further indicate that tight control of miR expression levels is required in regulating class specific dendritic architecture. In particular, our miR-specific gain-of-function analyses implicate *miR-12* as the primary regulator with respect to the formation of actin-rich dendritic sensory filopodia and demonstrate that regulated expression of *miR-12* is critical in establishing class-specific dendritic architectures as overexpression of *miR-12* in class IV neurons leads to a morphological shift towards architectures that are normally observed exclusively in class III neurons (i.e. dendritic filopodia). Bioinformatic and target gene analyses indicate that the *miR-12/283/304* cluster regulates the expression of genes associated with dendritic development and actin cytoskeletal organization. Moreover, our analyses demonstrate that *miR-12* acts to reorganize the actin cytoskeleton specifically thereby revealing one potential mechanism by which this miR contributes to the refinement of class-specific dendritic architectures. At a target gene level, we have validated two *miR-12* targets including the genes *Pka-C1* and *Syb*. Knockdown of these molecules in class IV neurons leads to *de novo* formation of dendritic filopodia suggesting that proteins act to repress formation of sensory filopodia. *Syb*, also known as *VAMP*, has been demonstrated to function as a v-SNARE molecule (SNAP receptor activity) with important roles in synaptic vesicle docking and fusion events involved in exocytosis in neurons (Littleton, 2000), whereas *Pka-C1* encodes a cAMP-dependent protein kinase which functions as a

catalytic subunit of *Pka* which is restricted to neuronal tissue (Muller, 1997). Moreover, *Pka-C1* has been directly linked to the *hedgehog* (*hh*) signaling pathway (Therond et al., 1996) and repression of *dpp* signaling (Pan and Rubin, 1995). Taken together, these findings suggest that in dendrite development, repression of vesicular exocytosis and *hh* signal transduction may be required to promote the formation of dendritic filopodia.

Intriguingly, previous studies on the Hedgehog signaling pathway, that controls developmental processes such as differentiation, pattern formation and proliferation ranging from *Drosophila* to humans revealed that the mRNAs for *cos2*, *fu*, and *smo* can be regulated by a miRNA cluster including *miR-12* and *miR-283* in the *Drosophila* wing disc. Specifically, the overexpression of the miRNA cluster lowers the levels of *cos2*, *fu*, and *smo* mRNAs in addition to activating the Hedgehog pathway. However, loss-of-function analyses revealed modification of the 3'UTR of *smo* and *cos2*, along with other mRNAs contributing to Hedgehog components as physiological targets for these miRNAs (Friggi-Grelín et al., 2008). Moreover, studies performed in Honeybees designed to identify the correlation of differential expression of miRNA genes in the brain with age-dependent behavioral changes, revealed that *miR-12* and *miR-283* were upregulated in older forager bees, whereas the miRs *let-7* and *miR-124* were differentially expressed in the young nurse bees (Behura and Whitfield, 2010). *Drosophila miR-12* was likewise previously observed to be differentially expressed with respect to age-dependent brain neurodegeneration in *Drosophila* (Liu et al., 2012). In recent studies, ectopic *miR-12* overexpression was shown to induce both strong vein thickening and wing notching in *Drosophila*, suggesting a potential relevance to regulation of the Notch signaling pathway (Bejarano et al., 2012). Moreover, investigation of miRNAs in mosquito and *Drosophila*

revealed that *miR-283* acts as the major regulator of developmental genes (Behura et al., 2011) and a differentially expressed mosquito *aae-miR-12* infected with *Wolbachia* targeted 2 genes MCM6 and MCT1 both of which must be negatively regulated by *aae-miR-12* in order to facilitate the replication/maintenance of *Wolbachia* in host cells (Osei-Amo et al., 2012).

The most conserved miRNAs among nematodes, flies and humans are likely to regulate biological functions that are likewise conserved between invertebrates and vertebrates. For example, *dme-miR-12* is evolutionarily conserved between nematodes, *Drosophila* and humans. Moreover, approximately 80 *Drosophila* microRNAs have human homologs, such as *dme-miR-12* and *dme-miR-283* have 5' sequence homology with *hsa-miR-496* and *dme-miR-304* has 5' sequence homology with *hsa-miR-216a* (Ibáñez-Ventoso et al., 2008). Given this strong evolutionary conservation, miRNome-wide functional studies in *Drosophila* have the potential to shed significant and novel insights into the mechanisms by which miRNAs exert control over biological processes of interest as well as potentially revealing mechanisms via which miRNA dysfunction may contribute to disease regulation (Ibáñez-Ventoso et al., 2008).

Collectively, these studies provide both global insight and a robust foundation on the importance of miRNAs in mediating class specific dendrite morphogenesis and will potentially shed novel light on the molecular mechanisms via which miRNA regulation underscores such biologically relevant events as learning and memory, as well as nervous system disease pathologies.

LIST OF REFERENCES

1. Abdelilah-Seyfried, S., Chan, Y.M., Zeng, C., Justice, N.J., Younger-Shepherd, S., Sharp, L.E., Barbel, S., Meadows, S.A., Jan, L.Y. and Jan, Y.N. (2000). A gain-of-function screen for genes that affect the development of the *Drosophila* adult external sensory organ. *Genetics* 155, 733-752.
2. Aboobaker, A.A., Tomancak, P., Patel, N., Rubin, G.M., and Lai, E.C. (2005). *Drosophila* microRNAs exhibit diverse spatial expression patterns during embryonic development. *Proc. Natl. Acad. Sci. U. S. A.* 102, 18017–18022.
3. Andersen, R., Li, Y., Resseguie, M., and Brenman, J.E. (2005). Calcium/calmodulin-dependent protein kinase II alters structural plasticity and cytoskeletal dynamics in *Drosophila*. *J. Neurosci. Off. J. Soc. Neurosci.* 25, 8878–8888.
4. Arikath, J. (2012). Molecular mechanisms of dendrite morphogenesis. *Front. Cell. Neurosci.* 6, 61.
5. Behura, S.K., and Whitfield, C.W. (2010). Correlated expression patterns of microRNA genes with age-dependent behavioural changes in honeybee. *Insect Mol. Biol.* 19, 431–439.
6. Behura, S.K., Haugen, M., Flannery, E., Sarro, J., Tessier, C.R., Severson, D.W., and Duman-Scheel, M. (2011). Comparative Genomic Analysis of *Drosophila melanogaster* and Vector Mosquito Developmental Genes. *PLoS ONE* 6, e21504.
7. Bejarano, F., Bortolamiol-Becet, D., Dai, Q., Sun, K., Saj, A., Chou, Y.-T., Raleigh, D.R., Kim, K., Ni, J.-Q., Duan, H., et al. (2012). A genome-wide transgenic resource for conditional expression of *Drosophila* microRNAs. *Development* 139, 2821–2831.
8. Bian, S., and Sun, T. (2011). Functions of noncoding RNAs in neural development and neurological diseases. *Mol. Neurobiol.* 44, 359–373.
9. Bodmer, R., and Jan, Y.N. (1987). Morphological differentiation of the embryonic peripheral neurons in *Drosophila*. *Roux Arch. Dev. Biol.* 196, 69–77.

10. Brand, A.H., and Perrimon, N. (1993). Targeted gene expression as a means of altering cell fates and generating dominant phenotypes. *Dev. Camb. Engl.* *118*, 401–415.
11. Calabrese, B., Wilson, M.S., and Halpain, S. (2006). Development and Regulation of Dendritic Spine Synapses. *Physiology* *21*, 38–47.
12. Calin, G.A., Dumitru, C.D., Shimizu, M., Bichi, R., Zupo, S., Noch, E., Aldler, H., Rattan, S., Keating, M., Rai, K., et al. (2002). Frequent deletions and down-regulation of micro- RNA genes miR15 and miR16 at 13q14 in chronic lymphocytic leukemia. *Proc. Natl. Acad. Sci. U. S. A.* *99*, 15524–15529.
13. Carthew, R.W., and Sontheimer, E.J. (2009). Origins and Mechanisms of miRNAs and siRNAs. *Cell* *136*, 642–655.
14. Chabu, C. and Doe, C.Q. (2008). Dap160/intersectin binds and activates aPKC to regulate cell polarity and cell cycle progression. *Development* *135*, 2739–2746.
15. Cochella, L., and Hobert, O. (2012). Diverse functions of microRNAs in nervous system development. *Curr. Top. Dev. Biol.* *99*, 115–143.
16. Conde, C., and Cáceres, A. (2009). Microtubule assembly, organization and dynamics in axons and dendrites. *Nat. Rev. Neurosci.* *10*, 319–332.
17. Davis, B.N., and Hata, A. (2009a). Regulation of MicroRNA Biogenesis: A miRiad of mechanisms. *Cell Commun. Signal. CCS* *7*, 18.
18. Duan, R., and Jin, P. (2006). Identification of messenger RNAs and microRNAs associated with fragile X mental retardation protein. *Methods Mol. Biol. Clifton NJ* *342*, 267–276.
19. Duffy, J.B. (2002). GAL4 system in *Drosophila*: a fly geneticist's Swiss army knife. *Genes. N. Y. N* *2000* *34*, 1–15.
20. Dutta, D., Bloor, J.W., Ruiz-Gomez, M., VijayRaghavan, K., and Kiehart, D.P. (2002). Real-time imaging of morphogenetic movements in *Drosophila* using Gal4-UAS-driven expression of GFP fused to the actin-binding domain of moesin. *Genesis* *34*, 146–151.
21. Edwards, K.A., Demsky, M., Montague, R.A., Weymouth, N., and Kiehart, D.P. (1997). GFP-moesin illuminates actin cytoskeleton dynamics in living tissue and demonstrates cell shape changes during morphogenesis in *Drosophila*. *Dev. Biol.* *191*, 103–117.

22. Enright, A.J., John, B., Gaul, U., Tuschl, T., Sander, C., and Marks, D.S. (2003). MicroRNA targets in *Drosophila*. *Genome Biol.* 5, R1.
23. Filipowicz, W., Bhattacharyya, S.N., and Sonenberg, N. (2008). Mechanisms of post-transcriptional regulation by microRNAs: are the answers in sight? *Nat. Rev. Genet.* 9, 102–114.
24. Fischer, J.A., Giniger, E., Maniatis, T., and Ptashne, M. (1988). GAL4 activates transcription in *Drosophila*. *Nature* 332, 853–856.
25. Friggi-Grelín, F., Lavenant-Staccini, L., and Therond, P. (2008). Control of antagonistic components of the hedgehog signaling pathway by microRNAs in *Drosophila*. *Genetics* 179, 429–439.
26. Gao, F.-B., Brenman, J.E., Jan, L.Y., and Jan, Y.N. (1999). Genes regulating dendritic outgrowth, branching, and routing in *Drosophila*. *Genes Dev.* 13, 2549–2561.
27. Gautier, L., Cope, L., Bolstad, B.M. and Irizarry, R.A. (2004). affy--analysis of Affymetrix GeneChip data at the probe level. *Bioinformatics* 20, 307–315.
28. Gennarino, V.A., Sardiello, M., Avellino, R., Meola, N., Maselli, V., Anand, S., Cutillo, L., Ballabio, A. and Banfi, S. (2009). MicroRNA target prediction by expression analysis of host genes. *Genome Res* 19, 481–490.
29. Gennarino, V.A., Sardiello, M., Mutarelli, M., Dharmalingam, G., Maselli, V., Lago, G. and Banfi, S. (2011). HOCTAR database: A unique resource for microRNA target prediction. *Gene* 480, 51–58.
30. Giniger, E., Varnum, S.M., and Ptashne, M. (1985). Specific DNA binding of GAL4, a positive regulatory protein of yeast. *Cell* 40, 767–774.
31. Giraldez, A.J., Cinalli, R.M., Glasner, M.E., Enright, A.J., Thomson, J.M., Baskerville, S., Hammond, S.M., Bartel, D.P., and Schier, A.F. (2005). MicroRNAs Regulate Brain Morphogenesis in Zebrafish. *Science* 308, 833–838.
32. Grueber, W.B., Jan, L.Y., and Jan, Y.N. (2002). Tiling of the *Drosophila* epidermis by multidendritic sensory neurons. *Dev. Camb. Engl.* 129, 2867–2878.
33. Grueber, W.B., Ye, B., Moore, A.W., Jan, L.Y., and Jan, Y.N. (2003). Dendrites of Distinct Classes of *Drosophila* Sensory Neurons Show Different Capacities for Homotypic Repulsion. *Curr. Biol.* 13, 618–626.

34. Grueber, W.B., Yang, C.-H., Ye, B., and Jan, Y.-N. (2005). The Development of Neuronal Morphology in Insects. *Curr. Biol.* 15, R730–R738.
35. Grueber, W.B., Ye, B., Yang, C.-H., Younger, S., Borden, K., Jan, L.Y., and Jan, Y.-N. (2007). Projections of *Drosophila* multidendritic neurons in the central nervous system: links with peripheral dendrite morphology. *Development* 134, 55–64.
36. Huang, D.W., Sherman, B.T., Tan, Q., Collins, J.R., Alvord, W.G., Roayaei, J., Stephens, R., Baseler, M.W., Lane, H.C. and Lempicki, R.A. (2007). DAVID gene functional classification tool: a novel biological module-centric algorithm to functionally analyze large gene lists. *Genome Biol.* 8, R183.
37. Huang, Y., Shen, X.J., Zou, Q., Wang, S.P., Tang, S.M., and Zhang, G.Z. (2011). Biological functions of microRNAs: a review. *J. Physiol. Biochem.* 67, 129–139.
38. Hughes, C.L., and Thomas, J.B. (2007). A Sensory Feedback Circuit Coordinates Muscle Activity in *Drosophila*. *Mol. Cell. Neurosci.* 35, 383–396.
39. Ibáñez-Ventoso, C., Vora, M., and Driscoll, M. (2008). Sequence Relationships among *C. elegans*, *D. melanogaster* and Human microRNAs Highlight the Extensive Conservation of microRNAs in Biology. *PLoS ONE* 3, e2818.
40. Ivanov, A.I., Rovescalli, A.C., Pozzi, P., Yoo, S., Mozer, B., Li, H.-P., Yu, S.-H., Higashida, H., Guo, V., Spencer, M., et al. (2004). Genes required for *Drosophila* nervous system development identified by RNA interference. *Proc. Natl. Acad. Sci. U. S. A.* 101, 16216–16221.
41. Iyer, E.P.R., Iyer, S.C., Sulkowski, M.J., and Cox D.N. (2009). Isolation and purification of *Drosophila* peripheral neurons by magnetic bead sorting. *J. Vis. Exp.* 34:e1599, doi: 10.3791/1599.
42. Iyer E.P.R., Iyer S.C., Sullivan L., Wang D., Meduri, R., Graybeal L.L, and Cox D.N. (2013). Functional genomic analyses of two morphologically distinct classes of *Drosophila* sensory neurons: Post-mitotic roles of transcription factors in dendritic patterning. *PLoS ONE* 8(8): e72434. doi:10.1371/journal.pone.0072434.
43. Jan, Y.-N., and Jan, L.Y. (2010). Branching out: mechanisms of dendritic arborization. *Nat. Rev. Neurosci.* 11, 316–328.
44. Jenett, A., Rubin, G.M., Ngo, T.-T.B., Shepherd, D., Murphy, C., Dionne, H., Pfeiffer, B.D., Cavallaro, A., Hall, D., Jeter, J., et al. (2012). A GAL4-Driver Line Resource for *Drosophila* Neurobiology. *Cell Rep.* 2, 991–1001.

45. Joshi, S.R., McLendon, J.M., Comer, B.S., and Gerthoffer, W.T. (2011). MicroRNAs-control of essential genes: Implications for pulmonary vascular disease. *Pulm. Circ.* *1*, 357–364.
46. Kao, C.-F., and Lee, T. (2012). Generation of Standard Wild-Type MARCM Clones for Analysis of Drosophila Brain Development. *Cold Spring Harb. Protoc.* *2012*, pdb.prot071662.
47. Karpova, N., Bobinnec, Y., Fouix, S., Huitorel, P., and Debec, A. (2006). Jupiter, a new Drosophila protein associated with microtubules. *Cell Motil. Cytoskeleton* *63*, 301–312.
48. Kaufmann, W.E., and Moser, H.W. (2000). Dendritic Anomalies in Disorders Associated with Mental Retardation. *Cereb. Cortex* *10*, 981–991.
49. Kaur, P., Armugam, A., and Jeyaseelan, K. (2012). MicroRNAs in Neurotoxicity. *J. Toxicol.* *2012*, 1–15.
50. Kertesz, M., Iovino, N., Unnerstall, U., Gaul, U., and Segal, E. (2007). The role of site accessibility in microRNA target recognition. *Nat. Genet.* *39*, 1278–1284.
51. Kiriakidou, M., Tan, G.S., Lamprinaki, S., Planell-Saguer, M.D., Nelson, P.T., and Mourelatos, Z. (2007). An mRNA m7G Cap Binding-like Motif within Human Ago2 Represses Translation. *Cell* *129*, 1141–1151.
52. Koizumi, K., Higashida, H., Yoo, S., Islam, M.S., Ivanov, A.I., Guo, V., Pozzi, P., Yu, S.-H., Rovescalli, A.C., Tang, D., et al. (2007). RNA interference screen to identify genes required for Drosophila embryonic nervous system development. *Proc. Natl. Acad. Sci.* *104*, 5626–5631.
53. Korobova, F., and Svitkina, T. (2010). Molecular Architecture of Synaptic Actin Cytoskeleton in Hippocampal Neurons Reveals a Mechanism of Dendritic Spine Morphogenesis. *Mol. Biol. Cell* *21*, 165–176.
54. Kraut, R., Menon, K. and Zinn, K. (2001). A gain-of-function screen for genes controlling motor axon guidance and synaptogenesis in Drosophila. *Curr. Biol.* *11*, 417–430.
55. Leaman, D., Chen, P.Y., Fak, J., Yalcin, A., Pearce, M. et al. (2005). Antisense-mediated depletion reveals essential and specific functions of microRNAs in Drosophila development. *Cell* *121*, 1097–1108.

56. Lee, T., and Luo, L. (1999). Mosaic analysis with a repressible cell marker for studies of gene function in neuronal morphogenesis. *Neuron* 22, 451–461.
57. Lee, T., and Luo, L. (2001). Mosaic analysis with a repressible cell marker (MARCM) for *Drosophila* neural development. *Trends Neurosci.* 24, 251–254.
58. Lee, T., Winter, C., Marticke, S.S., Lee, A., and Luo, L. (2000). Essential Roles of *Drosophila* RhoA in the Regulation of Neuroblast Proliferation and Dendritic but Not Axonal Morphogenesis. *Neuron* 25, 307–316.
59. Lewis, B.P., Shih, I., Jones-Rhoades, M.W., Bartel, D.P., and Burge, C.B. (2003). Prediction of mammalian microRNA targets. *Cell* 115, 787–798.
60. Littleton, J.T. (2000). A genomic analysis of membrane trafficking and neurotransmitter release in *Drosophila*. *J Cell Biol* 150, F77-82.
61. Liu, N., Landreh, M., Cao, K., Abe, M., Hendriks, G.-J., Kennerdell, J.R., Zhu, Y., Wang, L.-S., and Bonini, N.M. (2012). The microRNA miR-34 modulates ageing and neurodegeneration in *Drosophila*. *Nature* 482, 519–523.
62. Lugli, G., Larson, J., Martone, M.E., Jones, Y., and Smalheiser, N.R. (2005). Dicer and eIF2c are enriched at postsynaptic densities in adult mouse brain and are modified by neuronal activity in a calpain-dependent manner. *J. Neurochem.* 94, 896–905.
63. Luikart, B.W., Perederiy, J.V., and Westbrook, G.L. (2012). Dentate gyrus neurogenesis, integration and microRNAs. *Behav. Brain Res.* 227, 348–355.
64. McDonald, J.A., Khodyakova, A., Aranjuez, G., Dudley, C. and Montell, D.J. (2008). PAR-1 kinase regulates epithelial detachment and directional protrusion of migrating border cells. *Curr. Biol.* 18, 1659-1667.
65. Min, H., and Yoon, S. (2010). Got target?: computational methods for microRNA target prediction and their extension. *Exp. Mol. Med.* 42, 233–244.
66. Muller, U. (1997). Neuronal cAMP-dependent protein kinase type II is concentration in mushroom bodies of *Drosophila melanogaster* and the honeybee *Apis mellifera*. *J. Neurobiol.* 33, 33-44.
67. Osei-Amo, S., Hussain, M., O'Neill, S.L., and Asgari, S. (2012). Wolbachia-Induced aae-miR-12 miRNA Negatively Regulates the Expression of MCT1 and MCM6 Genes in Wolbachia-Infected Mosquito Cell Line. *PLoS ONE* 7, e50049.

68. Ou, Y., Chwalla, B., Landgraf, M., and Meyel, D.J. van (2008). Identification of genes influencing dendrite morphogenesis in developing peripheral sensory and central motor neurons. *Neural Develop.* 3, 16.
69. Pan, D. and Rubin, G.M. (1995). cAMP-dependent protein kinase and hedgehog act antagonistically in regulating decapentaplegic transcription in *Drosophila* imaginal discs. *Cell* 80, 543-52.
70. Parkinson, H., Kapushesky, M., Shojatalab, M., Abeygunawardena, N., Coulson, R., Farne, A., Holloway, E., Kolesnykov, N., Lilja, P., Lukk, M., Mani, R., Rayner, T., Sharma, A., William, E., Sarkans, U. and Brazma, A. (2007). ArrayExpress - a public database of microarray experiments and gene expression profiles. *Nucleic Acids Res.* 35, D747-750.
71. Parrish, J.Z., Kim, M.D., Jan, L.Y., and Jan, Y.N. (2006). Genome-wide analyses identify transcription factors required for proper morphogenesis of *Drosophila* sensory neuron dendrites. *Genes Dev.* 20, 820-835.
72. Reinhart, B.J., Slack, F.J., Basson, M., Pasquinelli, A.E., Bettinger, J.C., Rougvie, A.E., Horvitz, H.R., and Ruvkun, G. (2000). The 21-nucleotide let-7 RNA regulates developmental timing in *Caenorhabditis elegans*. *Nature* 403, 901–906.
73. Rooij, E. van (2011). The Art of MicroRNA Research. *Circ. Res.* 108, 219–234.
74. Saugstad, J.A. (2010). MicroRNAs as effectors of brain function with roles in ischemia and injury, neuroprotection, and neurodegeneration. *J. Cereb. Blood Flow Metab. Off. J. Int. Soc. Cereb. Blood Flow Metab.* 30, 1564–1576.
75. Schmitter, D., Filkowski, J., Sewer, A., Pillai, R.S., Oakeley, E.J., Zavolan, M., Svoboda, P., and Filipowicz, W. (2006). Effects of Dicer and Argonaute down-regulation on mRNA levels in human HEK293 cells. *Nucleic Acids Res.* 34, 4801–4815.
76. Schratt, G.M., Tuebing, F., Nigh, E.A., Kane, C.G., Sabatini, M.E., Kiebler, M., and Greenberg, M.E. (2006). A brain-specific microRNA regulates dendritic spine development. *Nature* 439, 283–289.
77. Shi, Y., Zhao, X., Hsieh, J., Wichterle, H., Impey, S., Banerjee, S., Neveu, P., and Kosik, K.S. (2010). MicroRNA regulation of neural stem cells and neurogenesis. *J. Neurosci. Off. J. Soc. Neurosci.* 30, 14931–14936.

78. Song, J.-J., Smith, S.K., Hannon, G.J., and Joshua-Tor, L. (2004). Crystal structure of Argonaute and its implications for RISC slicer activity. *Science* 305, 1434–1437.
79. Song, X.-M., Yan, F., and Du, L.-X. (2006). [Components and assembly of RNA-induced silencing complex]. *Yi Chuan Hered. Zhongguo Yi Chuan Xue Hui Bian Ji* 28, 761–766.
80. Southall, T.D., Elliott, D.A., and Brand, A.H. (2008). The GAL4 System: A Versatile Toolkit for Gene Expression in *Drosophila*. *CSH Protoc.* 2008, pdb.top49.
81. Sturm, M., Hackenberg, M., Langenberger, D., and Frishman, D. (2010). TargetSpy: a supervised machine learning approach for microRNA target prediction. *BMC Bioinformatics* 11, 292.
82. Therond, P.P., Knight, J.D., Kornberg, T.B. and Bishop, J.M. (1996). Phosphorylation of the fused protein kinase in response to signaling from hedgehog. *Proc. Natl. Acad. Sci. USA* 93, 4224-8.
83. Wang, J., Haubrock, M., Cao, K.-M., Hua, X., Zhang, C.-Y., Wingender, E. and Li, J. (2011). Regulatory coordination of clustered microRNAs based on microRNA-transcription factor regulatory network. *BMC Systems Biology* 5:199.
84. Wightman, B., Ha, I., and Ruvkun, G. (1993). Posttranscriptional regulation of the heterochronic gene *lin-14* by *lin-4* mediates temporal pattern formation in *C. elegans*. *Cell* 75, 855–862.
85. Wu, J.S., and Luo, L. (2006). A protocol for mosaic analysis with a repressible cell marker (MARCM) in *Drosophila*. *Nat. Protoc.* 1, 2583–2589.
86. Xu, X.-L., Li, Y., Wang, F., and Gao, F.-B. (2008). The Steady-State Level of the Nervous-System-Specific MicroRNA-124a Is Regulated by dFMR1 in *Drosophila*. *J. Neurosci.* 28, 11883–11889.
87. Yu, W., and Lu, B. (2012). Synapses and Dendritic Spines as Pathogenic Targets in Alzheimer’s Disease. *Neural Plast.* 2012, 1–8.
88. Zheng, H., Fu, R., Wang, J.-T., Liu, Q., Chen, H., and Jiang, S.-W. (2013). Advances in the Techniques for the Prediction of microRNA Targets. *Int. J. Mol. Sci.* 14, 8179–8187.